PHASE DIAGRAMS OF LAURIC ACID, HEXANE AND THE IONIC LIQUID TRIHEXYL(TETRADECYL)PHOSPHONIUM CHLORIDE

by

Amro Alkhudair

Submitted in partial fulfilment of the requirements
for the degree of Master of Science

at

Dalhousie University
Halifax, Nova Scotia
August 2014

TABLE OF CONTENTS

LIST OF TABLES

LIST OF FIGURES

ABSTRACT

Mass and molar phase diagrams of lauric acid (LA), hexane and the ionic liquid (IL) trihexyl(tetradecyl)phosphonium chloride were developed at room temperature. The diagrams and experimental tie-lines were obtained for the water saturated IL. The biphasic system of IL and hexane was observed for LA mole fractions less than 0.015 in IL and 0.005 in hexane. The gradual addition of LA caused the biphasic system to become monophasic at a molar fraction just below 0.01 for LA and 0.03 for IL. Composition of mixtures that phase separated were determined by weight and gas chromatography. LA showed a solubilizing effect on the IL, since increased concentrations of the fatty acid caused an increase in the miscibility of IL with hexane. It was hypothesized that this happened due to a polar association of LA with IL at the positively charged phosphonium site. Using hexane to extract products of hydrolysis from the IL was deemed unsuitable due to the preferential distribution of LA in the IL, rather than the hexane. Phase diagrams of triglycerides in a similar system were suggested to investigate the suitability of the IL as a medium for acidolysis reactions.

LIST OF ABBREVIATIONS USED

[bmim] [PF_6]	1-Butyl-3-methylimidazolium hexafluorophosphate
[bmim] [BF_4]	1-Butyl-3-methylimidazolium tetrafluoroborate
[omim] [PF_6]	1-Methyl-3-octylimidazolium hexafluorophosphate
[P_{66614}] [Cl]	Trihexyl(tetradecyl)phosphonium chloride
[$P(h_3)t$] [Tf_2N]	Trihexyl(tetradecyl)phosphonium bis(trifluormethylsulfonyl) imide
DAG	Diglyceride
FAME	Fatty acid methyl ester
FFA	Free fatty acid
GC	Gas chromatography
HF	Hydrofluoric acid
HX	Hexane
IL	Ionic liquid
IS	Internal standard
LA	Lauric acid
LA FAME	Methyl laurate
MAG	Monoglyceride
TAG	Triglyceride
TLC	Thin-layer chromatography

ACKNOWLEDGMENTS

My sincerest appreciation cannot be expressed in words towards both my supervisor and co-supervisor, Dr. Gianfranco Mazzanti and Dr. Suzanne Budge. What seemingly felt like a never ending path driven in the dark was shimmered with light by bountiful, productive insight that helped build this Thesis. To Dr. Mazzanti, for not only being a supervisor but a friend as well in both the good and hard times; the epic proportion and wealth of knowledge bestowed by you is eternally treasured. To Dr. Budge for proposing the original idea and concept with enough enthusiasm that helped gather my attention and willingness to build it into my Thesis. For the patience that went with giving me "just a minute" more times than I can count, your positive push makes me want to see the "real" objective through. I humbly appreciate your help and concern through this journey. To my external supervisory committee member, Dr. J. Clyburne who gladly helped in answering any questions, provided the ionic liquid used in this study and gave plenty of useful insight throughout my research, I thank you.

I must express my deepest praise towards both groups of whom I have had the great pleasure to work with. A huge thanks to my colleagues in the "Mazzanti" group, in particular towards my lab mate Pavan K. Batchu; you are simply a legend. I thank you and Omar Al-Qatami for the great discussions and the shared laughs. To the Dalhousie marine oils laboratory, for being the cheerful and always helpful group that you are, I sincerely thank you. To Anas Aman, Mohamed Ismail, the Vadiee brothers (& family!), Baradah and the many friends across the world who have always backed me up, your amity and camaraderie is truly cherished.

To both my sisters for having to put up with all the craziness and spontaneity of the "Animlè", your gathered support will forever be appreciated. Special credit goes to my brother; Khalid Alkhudair for being a continuing source of inspiration to myself and many others, I continue to look up to you. I must acknowledge my loving grandmother for the continued prayers aimed towards my success and well-being as well as further acknowledging my close uncles for being the thoughtful folks they are.

No acknowledgement can ever live up to the gratitude I have towards both my selfless parents; Dr. Waleed Alkhudair and Dr. Kholoud Aljiboury who have never showed an iota in lack of support and love. For the never hindered belief that I would overcome and make it through, simply put, you are the reason I ALWAYS make it through. I dedicate this Thesis to the both of you.

Finally, it is only by the mercy and grace of Allah that I can achieve anything. I believe nothing would be possible otherwise.

"He who makes a beast of himself gets rid of the pain of being a man" – Dr. Johnson

CHAPTER 1 INTRODUCTION

The hydrolysis of triglycerides (TAGs) is not only an important process in the human body, it is also a reaction that helps yield free fatty acids (FFA) for use in a variety of industrial applications. Industrial operations account for 16 million tons of FFA produced every year (Murty et al., 2002). Soaps, detergents, cosmetics and many other products are composed largely of FFA (Ngaosuwan et al., 2009). To carry out the industrial hydrolysis reactions of TAGs, three techniques are currently used:

1) Fat splitting. This is the most commonly used practice in the industry today (Ackelsberg, 1958). Carried out at extremely high temperatures and pressure, the process is exceedingly energy intensive and expensive to maintain, spurring research to find alternatives (Ngaosuwan et al., 2009; Yow & Liew, 1999).

2) Chemically catalyzed hydrolysis. These reactions are usually carried out by saponification of TAGs with a strong base in an ethanol solution (Bucolo & David, 1973).

3) Enzymatically catalyzed hydrolysis. Typically carried out at temperatures slightly above ambient conditions, lipases are dispersed in aqueous solutions with TAGs to form liquid –liquid dispersions (Murty et al., 2002).

The advantages that enzymatic reactions have over chemical catalysts have been thoroughly reviewed (Ghaly et al., 2010). Chiefly, lower temperature and lower energy consumptions compared to both the chemically catalyzed hydrolysis and the fat splitting method make enzymatic catalysis a better method (Ghaly et al., 2010; Serri et al., 2008).

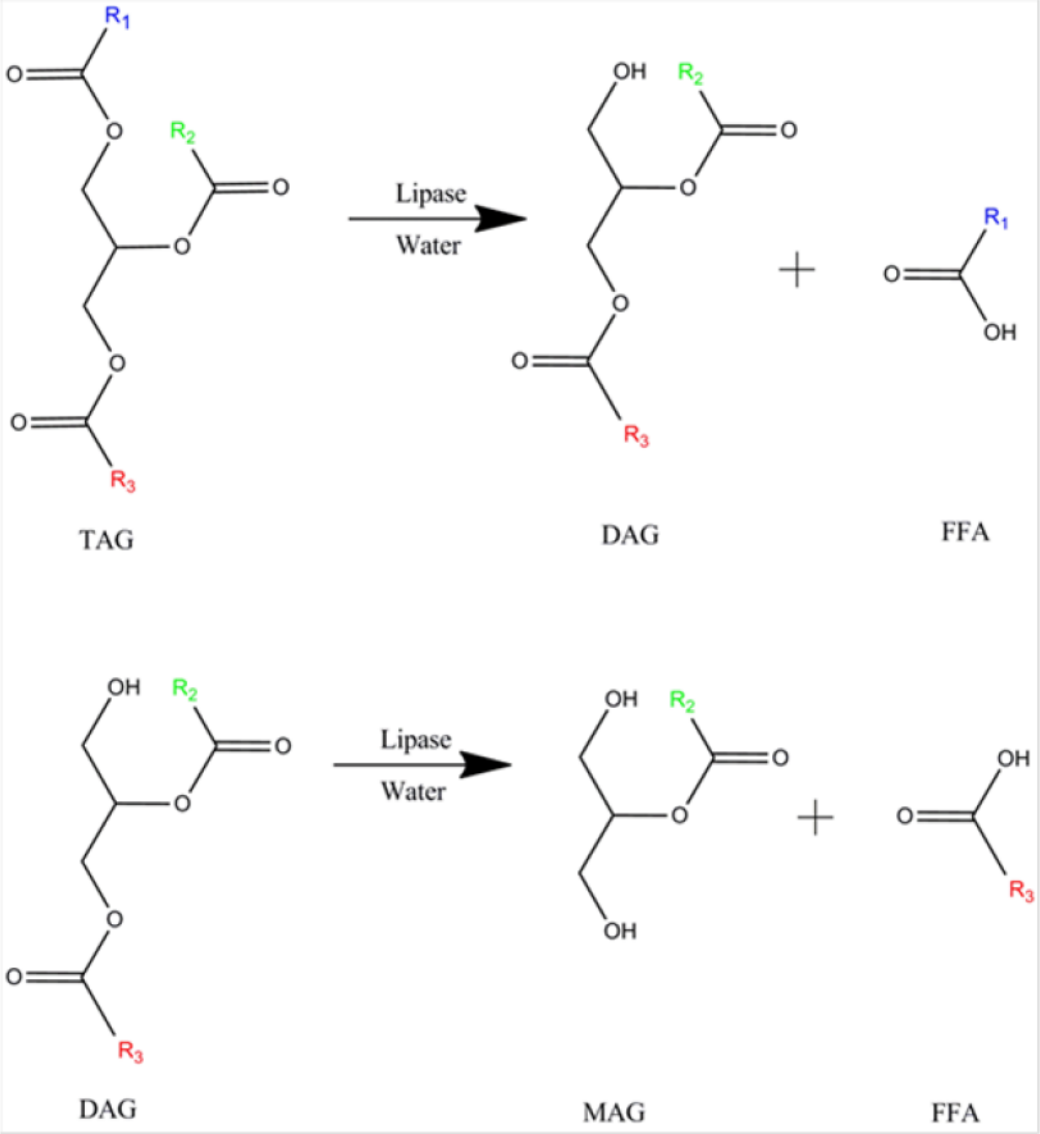

Figure 1-1: Reaction scheme of the enzymatically catalyzed hydrolysis reaction of a TAG to a MAG.

The hydrolysis of the ester bond and the glycerol moiety of a TAG results in a diglyceride (DAG) and FFA (Figure 1-1). The figure also illustrates the continued enzymatic hydrolysis of DAG yielding a monoglyceride (MAG) and an additional FFA as a result. The successful completion of a reaction depends on multiple factors such as temperature, concentration of substrates and time (Hamam & Shahidi, 2005). Enzymes have been immobilized rather than used in their free form to improve their recovery. At the

forefront of their advantages is the ability to reuse them for more than one reaction cycle (Iso et al., 2001). However, immobilized enzymes carry the disadvantage that they are much more expensive than free enzymes (Tischer & Wedekind, 1999).

With this knowledge, a method was proposed to retain free enzymes using a fluid supportive medium that would allow successive reactions. The medium chosen for this purpose was an ionic liquid (IL) which has seen an incredible boom in research for its potential in chemical innovations (Rogers & Seddon, 2003). These liquids are capable of withstanding high temperatures necessary for optimal enzyme conditions. They also comprise a wide range of solubility levels with other liquids, allowing them to form biphasic or even triphasic mixtures. Finally, these liquids have the prospective of saving money if the proposed method to immobilize free enzymes within them for use in successive reactions was to succeed.

A number of studies have been done regarding the use of enzymatic reactions in ILs (e.g., Kragl et al., 2002; Zhao et al., 2002). The majority of the research has focused on the viability and increase of product yields from reactions conducted in IL using enzymes immobilized on a solid support, compared to corresponding work done in organic solvents (Lau et al., 2000). That is, ILs have been considered mainly for their potential as "environmentally conscious" substitutes to organic solvents when in reality not all ILs have been found to be "green" (Abu-Eishah, 2011; Atefi et al., 2009; Sowmiah et al., 2009). The variety of potential enzymatic reactions in ILs has gained a large body of interest. Sheldon et al. (2002) showed that the enzyme *Candida antarctica* lipase B in both free and immobilized forms was able to catalyze different reactions in the ILs 1-butyl-3-methylimidazolium hexafluorophosphate ([bmim] $[PF_6]$) and 1-butyl-3-

methylimidazolium tetrafluoroborate ([bmim] [BF_4]) without the addition of water. It was noted that the immobilized enzyme performed better than the free enzyme in both ILs. However, these two particular ILs containing fluorine anions are very prone to hydrolysis when in contact with water, producing hydrofluoric acid (HF) (Freire et al., 2010; Stojanovic et al., 2010). Since water is required to hydrate free enzymes (H.Temme et al., 2012), such ILs may inhibit the enzyme from properly functioning by producing HF once in contact with water. H.Temme et al. (2012) found that using naringinase for hydrolysis of rutin in 23 different ILs was largely dependent on the solubility of the substrate in the IL and that the hydrophobic IL trihexyl(tetradecyl)phosphonium bis(trifluormethylsulfonyl) imide [$P(h_3)t$] [Tf_2N] was more suitable than other ILs as a medium for enzymatic reactions. Out of the 23 ILs, [$P(h_3)t$] [Tf_2N] showed the highest residual enzymatic activity whereas the lowest activity (lower than 3% conversion) was observed in the ILs that were miscible with water.

A method has been proposed in our research group where a free enzyme capable of catalyzing hydrolysis reactions is hydrated and IL is subsequently added. The oil selected to undergo hydrolysis is added to the IL and water, and the optimal conditions for the enzymatic reactions are provided (e.g. set temperatures, stirring via magnetic stirrer, etc.). After the hydrolysis reaction is complete, product recovery requires that TAGs, FFAs and all intermediates partition into an organic solvent added to the system. For the proposed process to be successful, the IL must contain the free enzymes after the reaction and the majority of the product must be easily extracted by the organic solvent so that subsequent reactions can be performed using the same enzymes.

A trial enzymatic hydrolysis reaction of canola oil using a lipase powder (free enzyme) *Aspergillus niger* (Amano A) in the IL trihexyl(tetradecyl)phosphonium chloride ([P_{66614}] [Cl]) was performed and compared via thin-layer chromatography (TLC) to a control reaction of the same reagents and enzyme carried out in hexane. The extraction of the reaction products from the IL was carried out by adding hexane as a top layer above the IL and letting the hexane sit for 10 minutes before removing it (the full procedure for both enzymatic trials of the control and IL, as well as the preparation and use of TLC is described in Appendix A). Large yields of FFA signified a very successful hydrolysis reaction where many TAG molecules reacted, as seen in the control run (left) in Figure 1-2. However, only a small quantity of FFA was observed on the TLC plate corresponding to the experiment carried out in the IL (right). In both cases, the unreacted canola oil applied on both TLC plates showed an absence of FFA.

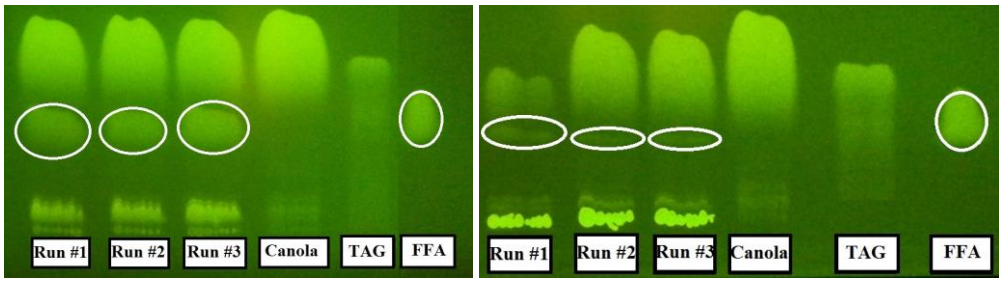

Figure 1-2: TLC silica plates showing a triplicate run of the enzymatically catalyzed hydrolysis reaction of canola oil along with standards. The light green bands highlighted with a white circle correspond to FFA produced via hydrolysis and to the respective standard. **Left**: Reaction done in hexane. **Right**: Reaction done in the IL [P_{66614}] [Cl].

As a result of these findings, two possibilities were considered. The first is that the IL is not a very suitable support medium for free enzymes to perform hydrolysis reactions since the yields were visibly low. The second, opposing possibility is that the IL is in fact a very capable support medium for free enzymes and corresponding reactions, and the limited recovery of FFA may be due to the failure of hexane to extract all the FFA produced

from hydrolysis. Therefore, it was necessary to construct phase diagrams of a system composed of a FA, IL and hexane to determine which possibility was correct. Such phase diagrams also permit the amount of FFA in the hexane phase to be predicted under a variety of concentrations and allow one to evaluate the suitability of IL as a medium for hydrolysis reactions, aiding the design of future experiments involving free enzymes.

1.1 Objectives

The objective of this study was to construct phase diagrams of lauric acid (LA), IL ([P_{66614}] [Cl]) and hexane at room temperature. The phase diagrams will help determine if hexane is suitable as an extracting solvent of LA from the IL and consequently, if it is an appropriate solvent to recover enzymatic catalyzed hydrolysis products from the IL.

CHAPTER 2 LITERATURE REVIEW

2.1 Ionic liquids (IL)

Today, ILs are referred to as liquids completely composed of ions that remain liquid at room temperature (Rogers & Seddon, 2003). However, there are several ILs that are not liquid at room temperature. An example is methyltri-n-butylammonium docusate, which remains solid below 40 °C (Davis & Fox, 2003). Therefore, the term room temperature ionic liquid (RTIL) has been coined to help avoid confusion. However, for the sake of simplicity, all ionic liquids will be termed IL herein and assumed to be liquid at room temperature. ILs have been gathering considerable attention in the "green" field of research and with valid reason (Freire et al., 2010). ILs have negligible vapor pressure rendering them potential replacements of volatile organic solvents that can be hazardous to human health (Cull et al., 2000; Sheldon, 2005; Wasserscheid & Keim, 2000). Approximately 600 different volatile organic compounds are used today, the different possible mixtures of cations and anions in ILs allow infinite IL combinations (Rogers & Seddon, 2003). The substantial number of combinations leads to many different uses, as does the variety of solubilities with organic substances (Gardas & João, 2009). This in turn allows a large number of possibilities where the IL can be used solely as a solvent medium for different reactions.

Different physical properties among ILs that have the same cation but different anion have been documented. Chowdury et al. (2008) produced phase diagrams of organic solvents, water and two phosphonium based ILs with different anions. Similar to the objective of this Thesis in the context of separation processes, the study was done to understand the phase behaviour of the ILs with different organic solvents in the presence

of water at room temperature. The results showed noticeable differences in solubility between the two ILs and the organic solvents, but partial miscibility between both the ILs with water. Therefore, ILs sharing a common cation do not necessarily share the same physical properties. Similarly, the IL 1-butyl-3-methylimidazolium hexafluorophosphate ([bmim][PF_6]) was found to be immiscible with water whereas 1-butyl-3-methylimidazolium tetrafluoroborate ([bmim][BF_4]), differing from the former only in the anion, was miscible with water (Davis & Fox, 2003). Therefore, ILs can be chosen based on the physical characteristics they possess to function in different applications, and if an IL does not have the needed properties, the anion can be modified to create an IL with the desired features.

Although a wide range of ILs exist, the majority of studies have been conducted on imidazolium based ILs and to a lesser extent, pyridinium based ILs (Stojanovic et al., 2011; Tseng et al., 2007). According to Davis and Fox (2003), in 2002, out of 83 publications on ILs from the Royal Society of Chemistry, American Chemical Society and Elsevier databases, 74 described work using imidazolium based ILs. Recent discoveries have highlighted the possible advantages of phosphonium based ILs over other ILs as they have been found to have greater thermal and chemical stability, as well as a huge variance in miscibility with solvents (Stojanovic et al., 2011). Furthermore, compared to most imidazolium based ILs, phosphonium based ILs are less expensive to manufacture (Ferreira et al., 2012).

2.1.1 [P_{66614}] [Cl]

[P_{66614}] [Cl] was the IL chosen for our experiments (Figure 2-1). One of the main reasons behind this choice of IL was because, unlike the frequently used imidazolium based ILs, it did not contain fluorine anions that would undergo hydrolysis in the presence of water to produce HF. Furthermore, there have been no reports of [P_{66614}] [Cl] undergoing hydrolysis in the presence of water to produce hydrogen chloride and it was therefore a more suitable IL for a system that requires water. As a hydrophobic IL, [P_{66614}] [Cl] is immiscible with water, has a density of 0.895 mg/ml and a molecular weight of 519.31 units (Stojanovic et al., 2010; Strem Chemicals Inc., 2014). The decomposition of [P_{66614}] [Cl] occurs at 350 °C under a nitrogen atmosphere (Fraser & MacFarlane, 2009). [P_{66614}] [Cl] is also one of the few ILs that can be purchased commercially in bulk which helps in the scale-up of any useful findings to an industrial application (Anderson et al., 2009).

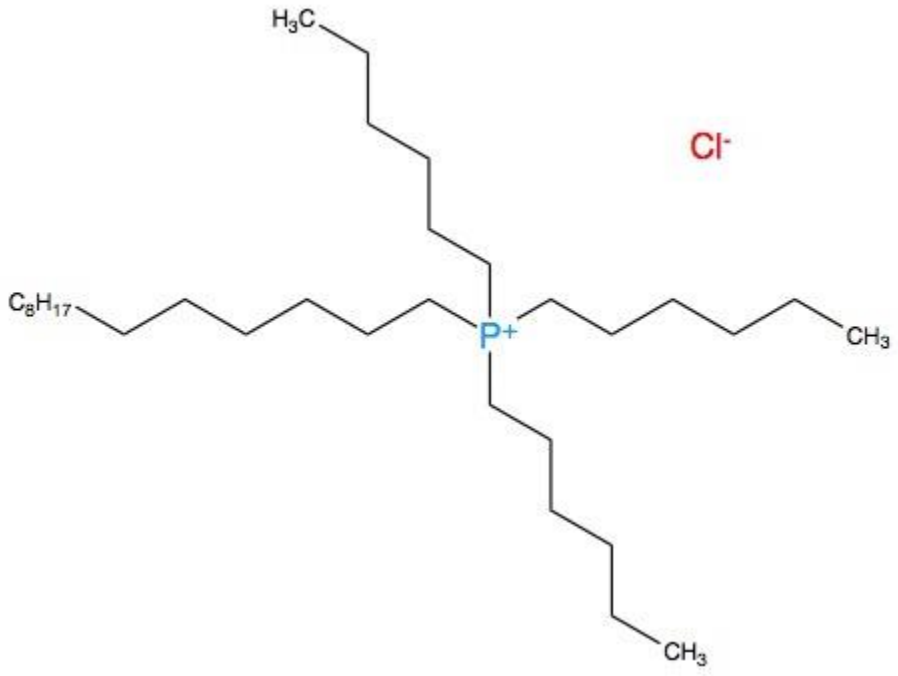

Figure 2-1: Molecular structure of [P_{66614}] [Cl].

Water and an organic solvent make a triphasic system with this IL, which should allow the isolation of a product of interest (Anderson et al., 2009). Water has been used to separate [P_{66614}] [Cl] ILs from saturated hydrocarbons (i.e. alkanes) (Earle et al., 2003). Since the objective of this study is to find the FFA distribution in the hexane phase and the [P_{66614}] [Cl] phase, adding water to the system to allow separation of hexane from the IL would prove valuable. By separating the hexane phase from [P_{66614}] [Cl], the hexane can be readily extracted along with the FFA settled within it. From the process invented by Earle et al. (2003), it is known that the presence of water above 15% w/v (water to IL) is sufficient to separate alkanes from the phosphonium IL (a single phase) and results in the formation of a more dense bottom aqueous phase and a less dense alkane layer at the top, with the IL forming a discreet third phase between the two. This separation is further enhanced if the alkane is hydrophobic or very nonpolar. Product isolation by the addition of water to an alkane and this particular IL is also noted in other work (Fraser & MacFarlane, 2009).

2.1.2 Phase behaviour of IL

Several studies have been conducted to determine the phase behavior of ILs with different organic solvents; however, as previously noted, most of the attention has been given to imidizolium based ILs and less data is available for phosphonium cations (Chen et al., 2008). Theoretical screening of solvents with ILs has been done by predictive tools such as COSMO-RS which uses results of quantum chemical calculations and statistical thermodynamics (Diedenhofen et al., 2003). Quantitative structure-property relationships or QSPR (Eike et al., 2004) and non-random two liquid segment activity coefficient models (NRTL-SAC) (Chen et al., 2008; Domańska & Królikowski, 2012) have also been used to

help predict the behavior of some ILs with organic solvents. Although different from our study in relation to the models used and scope, the quantity of studies on solvent interactions with ILs further highlights the interest and importance in understanding such interactions. Pàdua et al. (2007) showed various theoretical models of IL interactions at the molecular level and highlighted the importance of understanding such interactions at that scale as being the best way in which we may understand how ILs work.

Other ILs have been studied for their potential to be used as mediums for catalytic reactions through the construction of phase diagrams. Different analytical means such as gas chromatography (GC) and refractive index have been used to develop phase diagrams of IL, solvents and organic compounds (Chowdhury et al., 2008). Ternary liquid - liquid systems consisting of a number of ILs (excluding any phosphonium based ILs), hexane and several organic compounds have been investigated (Hernández-Fernández et al., 2008). The different compounds in the hexane rich phase were measured via GC whereas the quantity of compounds in the IL rich phase was found by refractive index. The purpose of the study was to determine the selectivity and subsequent extraction of the compounds via the solvent from the IL. The similarity of such work to ours stresses the importance of developing ternary phase diagrams that allow predictive extraction of organic compounds from an IL reaction mixture via a solvent. It also demonstrates the viability of using GC to measure the contents of the solvent layer to develop ternary phase diagrams of such systems.

Ternary phase diagrams of ILs, water and solvents have been constructed to help illustrate the different concentrations at which monophasic, biphasic and triphasic systems are observed. Similarly, studies have been conducted to determine the potential extraction

of a compound from the IL with different solvents. Ternary liquid-liquid phase diagrams of the IL [P_{66614}] [Cl], water and dodecane have been developed by Lago et al. (2012). The study was done to determine the suitability of [P_{66614}] [Cl] as a replacement for surfactants in enhanced recovery of oil in petroleum reservoirs. The phase diagrams showed a triphasic region composed of all three components and a biphasic region where the IL and dodecane assemble into a single phase, and the aqueous phase making up the other. The study determined the mass fractions of the three components when the different concentrations constituted either biphasic or triphasic systems. The authors concluded that the IL can in principle be used for enhanced oil recovery. However, the effect of adding the unspecified type of oil to the system of IL, dodecane and water was not conducted. Although the study is dissimilar in objective, where the potential of the IL to reduce the interfacial tension between water and oil by acting as a surfactant was evaluated, it helps shed light on the variety of potential applications that require ternary phase diagrams of the IL, water and solvent.

To a system composed of three liquids, equilibrium is needed to determine the solubility and the possible separation into different phases. Similarly, a triphasic system that is exposed to the addition of a different compound requires equilibration to ensure that the compound is allowed to settle in any of the phases at a concentration that is steady over time. Determination of the phase boundaries for a system made of [P_{66614}] [Cl], water and nonane conducted by Anderson et al. (2009) was carried out by agitating the system for a minute and then allowing it to sit undisturbed for 1-5 minutes. This technique was deemed sufficient to allow equilibration and enabled visible determination of the phases present. Several studies that sampled an IL [bmim] [PF_6], solvent and water used a methodology of

vortexing for 2 minutes followed by centrifuging for 2 minutes at 2000 g after each addition of solvent. The time frame and technique was assumed to be sufficient to reach equilibrium in the system (Visser et al., 2001; Visser et al., 2000). These studies helped provide a framework of conditions that should be sufficient to reach equilibrium in such systems.

2.2 Lauric acid (LA)

Dodecanoic acid, commonly known as lauric acid (LA), was chosen as the primary FA to be used in the experiments (Figure 2-2). Along with lesser amounts of myristic and capric acids, LA makes up the largest amount of TAGs found in coconut oil (Marina et al., 2009). LA is also the major FA found in palm kernel oil, making up approximately 48% of the composition (Young, 1983). LA has been studied within the bounds of the possible benefits of including it in the human diet (de Roos et al., 2001; E.Temme et al., 1999). LA was chosen because it is an inexpensive FA and was readily available in large quantity. The molecular weight of LA is 200.32 g/mol (Sigma-Aldrich, 2014a) and its density at room temperature was extrapolated from literature data and found to be 890 mg/ml (Noureddini et al., 1992). The solubility of LA in water at room temperature is reported as 4.8 mg/litre (Nyrén et al., 1958). For the purposes of this study LA solubility in water will therefore be considered negligible, and essentially all the LA will be in either the IL or organic solvent phase.

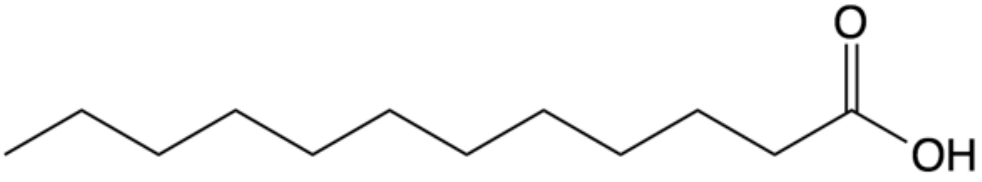

Figure 2-2: Molecular structure of LA.

2.3 Choice of solvent

A solvent for the system composed of IL, water and LA had to be chosen that suited our needs. The solvent must be effective in the extraction of products from a hydrolysis reaction. Such a solvent must also be nonpolar so as to be immiscible with water. This is important since water will be employed as the lower phase of the system and LA has negligible solubility in water. LA would therefore have to settle in either the IL or the organic solvent. Our solvent of choice should not be fully miscible with the IL either. By being entirely miscible with the IL, the ability to extract the product of a reaction is impeded since there would be no distinguishable layer to extract the solvent without extracting the IL.

Makowska et al. (2010) experimentally determined the liquid-liquid miscibility between $[P_{66614}]$ [Cl] and several alkanes. The results showed that the solubility with the IL decreased as the alkane chain length is increased. However, it is important to note that no aqueous phase was added to the system. Therefore, the process of separating the alkanes from the IL by adding a sufficient amount of water to the system above 15% w/v (water to IL) as described by Earle et al. (2003) was bypassed. Both studies by Lago et al. (2012), who used dodecane and Anderson et al. (2009) who used nonane are in agreement with the work done by Makowska et al. (2010). In the tests conducted by both research groups, the corresponding alkanes and $[P_{66614}]$ [Cl] without water showed a higher level of miscibility compared to when water was added to the system. However, the results also showed that dodecane had lower miscibility with the IL in the presence of water to that of nonane in a similar system. Thus, the higher hydrocarbon chain length of an alkane corresponds to a lower miscibility with the IL.

The employment of hexane as a potential extracting solvent in ILs other than [P_{66614}] [Cl] has been studied. Predictive extraction of different organic compounds including LA from the ILs [bmim] [PF_6] and 1-methyl-3-octylimidazolium hexafluorophosphate ([omim] [PF_6]) by the addition of hexane through supported liquid membranes has been conducted. The partition coefficient of LA between the ILs and hexane was reportedly very low for [bmim] [PF_6] but slightly higher for [omim] [PF_6]. As defined by the authors, the lower the partition coefficient, the lower the absorption in the IL (de los Ríos et al., 2008). Although the ILs used were different from [P_{66614}][Cl], the study illustrated the potential use of hexane as an extracting solvent of LA from the ILs and showed that a knowledge of predictive extraction is required to determine the suitability of both the solvent and IL for catalytic reactions.

The studies that show the theoretical potential of alkanes to be used as extracting solvents in [P_{66614}] [Cl] determined the solubility of the alkane with the IL but not the actual ability of the alkane to extract any compound from it. Although reported to have greater miscibility with [P_{66614}] [Cl] compared to alkanes with longer hydrocarbon chains, hexane has been previously used to extract products of a reaction from the IL. In a system of [P_{66614}] [Cl] and water, hexane was used to help form a triphasic mixture for product separation where the aqueous layer was at the bottom, IL in the middle and hexane at the top (Ramnial et al., 2005). Although products of a Grignard reaction, rather than FA, were isolated by the addition of hexane in the study, it was established that it is possible to extract a given product from this particular IL using hexane. Therefore, with the limited studies available for the extraction of products in a system made up of [P_{66614}] [Cl], water and organic solvents, hexane was chosen as the solvent for extracting LA from IL for several

reasons. Hexane is sufficiently nonpolar to be immiscible with water (Tsonopoulos & Wilson, 1983). LA has been shown to have a relatively good solubility in hexane (Cepeda et al., 2009; Hoerr & Harwood, 1951) and hexane has been used often to dissolve FAs (Tizol-Correa et al., 2006; Zaidi et al., 2002). Hexane has also been used in liquid – liquid extraction of FAs (Krygier et al., 1982) and is used extensively in industry to extract oils from vegetable sources. All these factors contributed in choosing hexane as the solvent for this study. The molecular weight of hexane is 86.18 g/mol (Sigma-Aldrich, 2014b), and its density at room temperature is 655 mg/ml (Aminabhavi et al., 1996).

Chloroform was considered as an alternate solvent as there is no reported literature on the behaviour of chloroform in such a system. Chloroform was also considered due to its polarity and its common use in extracting FFA (Iwata et al., 1992). Another common solvent for lipids is acetone, but it was not considered as a solvent of choice in our system. This is due to the reported high solubility of both the IL and water with acetone, which would likely result in a single phase system (Fu & Luthy, 1986; Stojanovic et al., 2010). Other common solvents for lipids, such as aromatic hydrocarbons, diethyl ether and propan-2-ol, are reported to be completely miscible with the IL and thus were not considered (Marták & Schlosser, 2006).

2.4 Fatty acid methyl esters (FAME)

Although LA could directly be analysed by GC, studies show that more reproducible data is obtained if the FA is derivatized into the more volatile fatty acid methyl ester (FAME) (David et al., 2005; Metcalfe & Schmitz, 1961). Many studies that have specifically converted LA into FAME for analysis in GC are available (Gao et al., 2009; Parfene et al., 2013). Acid, rather than base, catalyzed transesterification is necessary to

derivatize FA into FAME (Christie, 2002) and although several acid catalysts are capable of such transesterification, sulfuric acid is recommended most (Budge et al., 2006). In the presence of anhydrous methanol, heat and sulfuric acid, the FFAs are converted to LA FAME (Figure 2-3)

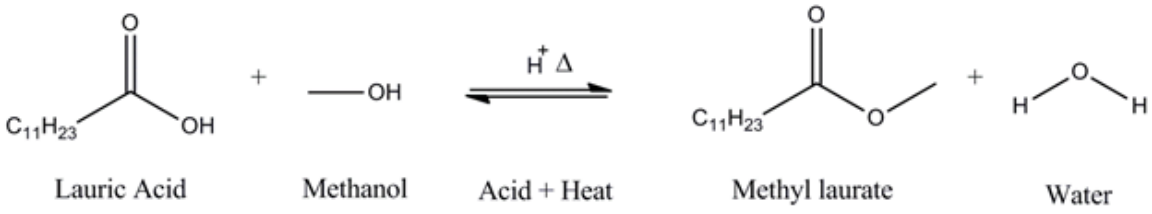

Figure 2-3: Acid catalyzed transesterification of LA to methyl laurate (LA FAME) in the presence of methanol, an acid and heat.

Several papers advise caution when evaporating solvent from mixtures containing short chain methyl esters via streaming nitrogen as the esters are sufficiently volatile to be lost in the process (Christie & Han, 2010; Christie, 2002; Clark & Bunch, 1997). As the experimental procedure presented here required the complete evaporation of solvents from samples containing the FAME of LA, and although LA is largely considered as a medium chain FA (albeit at the lower end of the spectrum) (Y. Chen et al., 2012), the percentage of possible losses must be found to ensure accurate analysis.

As traces of IL might be found in the extracted organic solvent layer detailed in the experimental procedure (3.2.2), the sample must be purified before subsequent analysis in GC. Easy options for purification of FAME include TLC or simple column chromatography using purchased ready-to-use cartridge columns packed with silica gel (Ghioni, Bell, & Sargent, 1996; Ichihara & Fukubayashi, 2010). The simplest procedure is to pass FAME in hexane through a Pasteur pipette plugged with glass wool and packed with silica gel as an adsorbent (Christie, 2002; Croes et al., 1997). A mixture of 80:20 v/v hexane: diethyl-ether solvent has also been used successfully to purify methyl esters before

GC analysis (Ibrahim & Ghannoum, 1996). This adsorbent is a precautionary but important step to take before readying samples for injection into a GC as not to clog the syringe or degrade the GC.

CHAPTER 3 MATERIALS AND METHODS

Several preliminary experiments were performed before establishing the final methods. Chloroform was evaluated as a possible solvent in IL and as a comparison to hexane (3.2.1.1). Experiments investigating the miscibility of hexane with IL were done to determine an acceptable amount of hexane needed to use (3.2.1.2). The "solubilizer effect" of LA was examined to help distinguish a region of interest of concentrations of LA/hexane to be mixed with IL (3.2.1.3). A test simulating conditions used in the experiment was also performed to evaluate the possible volatility and loss of LA FAME (methyl laurate) when evaporating the solvent to complete dryness (3.2.1.4). All experiments herein were: 1) conducted at room temperature; 2) the volume of water was maintained at 1 ml which proved to be large enough to always show a bottom aqueous phase; and 3) employed a pipetting technique of IL where a Pasteur pipette was inserted into another and the tip was broken so that it became wide enough to withdraw the highly viscous IL by suction.

3.1 Materials

Trihexyl(tetradecyl)phosphonium chloride [$P_{6\,6\,6\,14}$] [Cl] was kindly donated by Dr. Jason Clyburne, Department of Chemistry, Saint Mary's University (Halifax, NS). LA was purchased from Acros Organics with a purity level of ≥ 99% (Geel, Belgium). Methyl tricosanoate to be used as the internal standard (IS) and methyl laurate were bought from Nu-Check Prep, Inc. (Elysian, MN) with purity levels of >99%. All solvents and reagents (Optima grade), as well as silica gel (mesh size 14-20) and anhydrous sodium sulfate were purchased from Fischer Scientific (Fair Lawn, NJ). Glass wool was purchased from Sigma-Aldrich (Oakville, ON).

3.2 Methods

3.2.1 Preliminary experiments

3.2.1.1 Different solvent

To a 15 ml round bottom centrifuge test tube, 1 ml dH_2O and 1 ml IL were added followed by 1 ml of chloroform. The test tube was vortexed for a minute and centrifuged for 10 minutes (1640 rpm).

3.2.1.2 Hexane miscibility with IL

To four separate 10 ml graduated centrifuge conical bottom test tubes, 1.0 ml dH_2O was added, followed by 1.0 ml of IL. To each test tube, a different volume of hexane was added, starting at 1.0 ml and increasing by increments of 1.0 ml so that one test tube contained 1.0 ml hexane, 1.0 ml IL and 1.0 ml dH_2O. The second test tube contained 2.0 ml hexane, 1.0 ml IL + 1.0 ml dH_2O and so forth. The test tubes were then vortexed for a minute, followed by centrifugation for 10 minutes (1640 rpm). The volume level of the IL phase was then noted. A triplicate experiment similar to the one described above was conducted by adding 1.0 ml dH_2O, 1.0 ml IL by weight and 4.0 ml hexane. The samples were vortexed for one minute and centrifuged for 10 minutes (1640 rpm). The volume level of IL was noted.

3.2.1.3 LA effect

To six separate 10 ml graduated centrifuge conical bottom test tubes, 1.0 ml of dH_2O was added. This was followed with the addition of 1.0 ml of IL on top of the dH_2O. To five of the test tubes, 4.0 ml of different concentrations of LA dissolved in hexane were added (Table 3-1). The five concentrations ranged down a log scale and were prepared by

adding a specific amount of LA to hexane to make up the required concentration (e.g. 1 g LA +10 ml hexane = 100 mg/ml). The sixth test tube served as a blank by adding 4.0 ml of pure hexane without LA. Each test tube was vortexed for a minute, centrifuged for 10 minutes (1640 rpm) and then left to settle for 10 minutes. Observations on the IL level were then noted. The samples were left for 24 hrs and any variations thereafter were noted. The same experimental procedure was carried out using 4.0 ml of 9, 8 and 7 mg/ml concentrations of LA/hexane and the volume level of the IL phase was noted.

Table 3-1: Concentrations of LA/hexane added to 1.0 ml dH_2O +1.0 ml IL.

Run	LA/Hexane concentration (mg/ml)	Total LA in system (mg)
1	100	400
2	10	40
3	1	4
4	0.1	0.4
5	0.01	0.04
6	blank	0

3.2.1.4 LA FAME volatility

To a tared 20 ml round bottom test tube containing a known amount of LA FAME, 5 ml of hexane was added and then vortexed for a minute. The solvent was then evaporated using a water bath nitrogen evaporator (N-EVAP) (Berlin, MA) at 34 °C and a steady stream of nitrogen. The mass of the product was then determined by difference. This experiment was done in triplicate.

3.2.2 Ternary mixtures of LA + hexane + IL experimental method

All the following experiments were done in triplicate and at room temperature. Due to the high viscosity of the IL, it was difficult to measure a volume with great accuracy.

Instead, the mass of the IL added was measured to approximately coincide with the reported mass of 1 ml IL in the literature, 895 mg. The precise mass of IL in each experiment (to 0.1 mg) was noted for future reference.

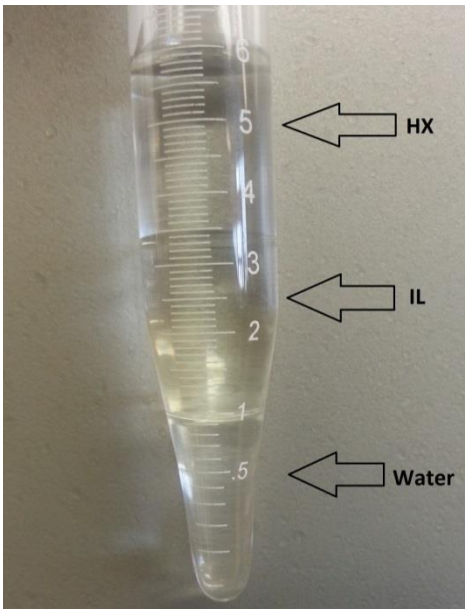

Figure 3-1: A triphasic system composed of 1.0 ml dH_2O, 1.0 ml IL and 4.0 ml hexane. The photograph was taken after equilibration by vortexing and centrifugation.

Series #1: To a 10 ml graduated (0.1 ml divisions) conical bottom centrifuge test tube, 1.0 ml dH_2O and 1.0 ml of IL were added. A starting concentration of LA dissolved in hexane (i.e. 4.0 ml of 1 mg/ml) was added (Table 3-2). The solutions of LA dissolved in hexane were made following the same methodology described in section 3.2.1.3 and the masses of LA were noted. The sample was vortexed for one minute, centrifuged for 10 minutes (1640 rpm) and then left to settle for an additional 10 minutes. The volume that the IL layer occupied was observed and noted (Figure 3-1). A 20 ml round bottom test tube with screw cap containing a known amount of the IS (methyl tricosanoate) was pre-weighed. Using the readings on the graduated test tube to serve as a guide, 1.0 ml of the top (hexane) layer was extracted and added to the pre-weighed test tube containing the IS.

The same volume (1.0 ml) of pure hexane was then added back to the graduated test tube to replenish the volume extracted. The test tube containing the sample was then placed in the water bath at 34 °C under a steady stream of nitrogen until the hexane evaporated. The weight was then noted as the mass of the test tube with the masses of IS, LA and IL. The FAME procedure detailed in section 3.2.3 was then performed. An additional 1.0 ml containing the concentration of LA in hexane as indicated in Table 3-2 (i.e. 10 mg/ml) was added to the graduated test tube containing the IL + LA + hexane and the entire procedure was repeated. Subsequently, the same procedure was performed on the series of concentrations shown in Table 3-2, resulting in a total of 4 extractions.

Table 3-2: Sequence of LA/hexane concentrations added to 1.0 ml of dH_2O and 1.0 ml IL in Series #1.

Series #1	**LA/Hexane concentration (mg/ml)**	**Volume LA/Hexane mixture added (ml)**
Starting Concentration	1	4
Addition #1	10	1
Addition #2	10	1
Addition #3	10	1
Total LA added (not corrected for LA removed)	34 (mg)	7

Series #2: To a separate graduated conical bottom centrifuge test tube, 1.0 ml dH_2O, 1.0 ml of IL and a starting concentration of LA dissolved in hexane shown in Table 3-3 were added. The same procedure described for Series #1 was performed.

Table 3-3: Sequence of LA/hexane concentrations added to 1.0 ml of dH_2O and 1.0 ml IL in Series #2.

Series #2	LA/Hexane concentration (mg/ml)	Volume LA/Hexane mixture added (ml)
Starting Concentration	10	4
Addition #1	20	1
Addition #2	20	1
Addition #3	20	1
Total LA added (not corrected for LA removed)	100 (mg)	7

Similarly, a blank experiment without LA was performed by adding 1.0 ml dH_2O, 1.0 ml IL and 4.0 ml hexane. After equilibration, 1.0 ml of the top phase was extracted and inserted into a pre-weighed test tube. The contents of the test tube were then placed under the water bath nitrogen evaporator at 34 °C until the solvent evaporated. The test tube was then weighed, and the mass of the IL noted.

3.2.3 FAME procedure

The extracted LA from the top layer of hexane was converted into FAME using acid-catalyzed esterification. Approximately 1.5 ml sulfuric acid was mixed with 100 ml methanol that had been dried by adding anhydrous sodium sulfate to make Hilditch reagent (Hilditch & Williams, 1964). 3.0 ml of Hilditch reagent and 1.5 ml of dichloromethane containing 0.01% BHT were added to the test tubes containing the extracted LA. The

samples were then flushed with nitrogen, capped and vortexed before being placed on a heating block at 100 °C for an hour. The samples were left to cool down to room temperature before adding 1.0 ml dH_2O and 3.0 ml hexane. The samples were then capped, vortexed and centrifuged for 2 minutes (1640 rpm). The top layer was extracted to a separate 10 ml centrifuge test tube. The extraction was repeated twice by adding 1.0 ml hexane to the first tube and following the same steps. 1 ml dH_2O was added to the second test tube containing the FAME in hexane and was capped, vortexed and centrifuged for 2 minutes (1640 rpm). The top layer was then removed to a third 10 ml centrifuge test tube to which a scoop of anhydrous sodium sulfate was added to remove any moisture.

3.2.4 Silica gel column

Since traces of IL were present in the hexane top layer, a procedure was devised to remove it before the GC step. For each FAME sample, a Pasteur pipette was used as a purifying column. The pipette was plugged with glass wool and packed tightly with silica gel that had been activated at 100 °C for an hour. The columns were pre-eluted with hexane. Pre-weighed 10 ml centrifuge test tubes were placed underneath each column (Figure 3-2). The liquid samples in the third 10 ml centrifuge test tubes (described in 3.2.3) with settled anhydrous sodium sulfate were then loaded onto the columns. 3 ml of a solvent mixture made of 80:20 v/v hexane: diethyl ether was used as the eluting solvent and added to the columns. After the samples and eluting solvents had run down the columns to the pre-weighed tubes, they were evaporated by being placed in the water bath at 34 °C under a stream of nitrogen. The total mass of FAME was then determined and hexane was added back to make up a concentration of 50 mg FAME/ml hexane. The samples were then transferred to GC vials, flushed with nitrogen and capped.

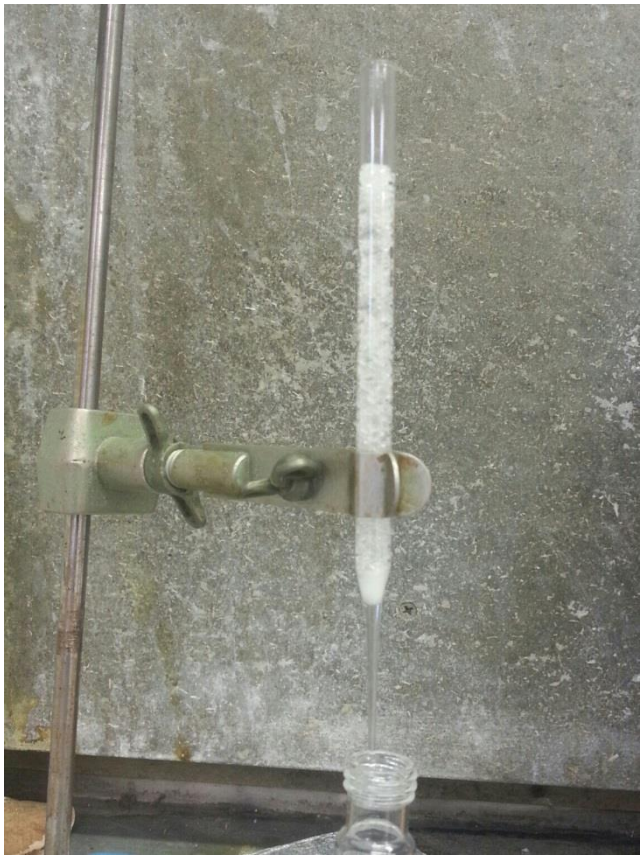

Figure 3-2: Silica gel column loaded with pre-elutant hexane, inserted into a 10 ml centrifuge test tube ready to be loaded with sample.

3.2.5 GC

The analysis of FAME samples was done on a Bruker Scion 436-GC instrument equipped with FID detector, CP-8400 Autosampler and a DB-23- high polarity column (30 m length, 0.250 mm diameter, 0.25 µm film) coated with 50% cyanopropyl polysiloxane. 1 µl of the FAME sample was inserted into the injector using a 5 µl syringe and was held at 250 °C before entering the gas phase. The split flow of helium was set at a rate of 100 ml/min, generating an approximate split ratio of 1:100. The initial temperature of 153 °C was held for 2 minutes and was increased at a rate of 2.3 °C/min to a temperature of 174 °C and held for 0.20 minutes. The temperature was then increased at a rate of 2.5 °C/min

to a final temperature of 205 °C and was held for 11 minutes. The detector was held at 270 °C (Budge et al., 2006).

3.3 Calculating the mixtures, top and bottom phases

Note: Although dH_2O was added and was always the bottom phase in all experiments, for our purposes in constructing the phase diagrams of IL, hexane and LA, water is excluded from all calculations and the IL rich phase will be considered as the bottom phase. Hexane will be abbreviated to HX here and in the results and discussion. To determine the mass and molar fractions needed to construct the phase diagrams, the masses of all 3 components must be determined.

Each experimental run was separated into 3 parts:

1) Mixture: Comprised of all the components initially added to the system, before equilibration.

2) Top phase: HX rich phase containing IL and LA that were found analytically.

3) Bottom phase: IL rich phase containing LA and HX that were found by mass balance.

For ease of explanation, an example of a run is detailed here. It is taken from Series #2 of experiments shown in Table 3-2 with a starting concentration of 10 mg/ml LA to HX and a 4.0 ml volume of the mixture added to 1.0 ml IL:

Mixture:

Equation 1

$$V_{LA} + V_{HX} = V_{added}$$

Where: V_{LA} = Volume of LA

V_{HX} = Volume of HX

V_{added} = Volume of the LA+HX concentration added to IL

The V_{added} in this example = 4.0 ml so either V_{LA} or V_{HX} must be found.

Equation 2

$$V = \frac{m}{\rho}$$

Where: V = volume

m = mass

ρ = density

By knowing the density (Table 3-4) and the mass of LA, the volume can be found.

While preparing the concentrations of LA in HX (3.2.2), the initial mass of LA added was noted and therefore the total mass of LA in 4.0 ml hexane was found:

$m_{\mathrm{LA(Total)}}$ = 40.12 mg

$$V_{LA}\,(\mathrm{ml}) = \frac{40.12\,\mathrm{mg}}{890\,\mathrm{mg/ml}} = 0.04508\,\mathrm{ml}$$

Following ***Equation 1***

4.0 ml – 0.04508 ml = 3.95 ml HX

$m_{HX\,(Total)}$ = 3.95 ml x 655 mg/ml = 2590.47 mg

The mass of IL was noted when added as described in 3.2.2

$$m_{IL\,(\mathrm{Total})} = 890.2\,\mathrm{mg} \qquad V_{IL} = \frac{890.2\,\mathrm{mg}}{895\,\mathrm{mg/ml}} = 0.99\,\mathrm{ml}$$

Table 3-4: Densities of the three main components in the experiment.

Component	Density in mg/ml
HX	655
LA	890
IL	895

Top phase:

The concentrations of LA in the "1 ml"[1] extracted from the top phase were calculated from peak areas given by the GC using the following equation:

Equation 3

$$m_{LAFAME(Coll)} = \frac{m_{IS} \times \left(\frac{A_{LA}}{A_{IS}} \right)}{CF}$$

Where: $m_{LAFAME(Coll)}$ = Mass of LA FAME in collected volume.

m_{IS} = Known mass of IS

A_{LA} = Peak area of LA FAME

A_{IS} = Peak area of IS

CF = Correction factor

A correction factor for the differential responses of the LA FAME and IS in the FID was added to all sample concentrations as detailed in Appendix B.

A conversion factor was also added to compensate for the additional mass of a CH_2 group in the LA FAME relative to mass of LA.

Equation 4

$$m_{LA(Coll)} = \frac{m_{LAFAME(Coll)} \times MW_{LA}}{MW_{LAFAME}}$$

[1] The "1 ml" has an uncertainty of approximately ± 0.05 ml from the divisions of the test tubes.

Where: MW_{LA} = Molecular weight of LA

MW_{LAFAME} = Molecular weight of LA FAME

Continuing with the example:

$m_{LA\ (Coll)}$ = 0.35 mg

As the volume collected = 1.0 ml $C_{LA\ (Coll)}$ = 0.35 mg/ml

The total $m_{LA(Top)}$ in the top phase is found by:

Equation 5

$$m_{\mathrm{LA(Top)}} = C_{LA(Coll)} \times V_{(Top\_T)}$$

Where: $V_{(Top\_T)}$ (ml) = total volume of the top phase.

$V_{(Top\_T)}$ was measured from the test tube scale by observing the partition between the top and the bottom phases. The graduated test tubes had 0.1 ml divisions and the measurement was done by eyesight.

$m_{LA\ (Top)}$ = 0.35 mg/ml x 1.9 ml

$m_{LA\ (Top)}$ = 0.67 mg

Equation 6

$$m_{\mathrm{LA(Coll)}} + m_{(T\_IS)} = m_{(T\_IS\_LA)}$$

Where: $m_{(T\_IS)}$ = Mass of pre-weighed test tube with IS described in 3.2.2.

$m_{(T\_IS\_LA)}$ = Mass of test tube, IS and LA.

Equation 7

$$m_{IL(Coll)} = m_{(T\_IS\_S)} - m_{(T\_IS\_LA)}$$

Where: $m_{IL(Coll)}$ = Mass of IL in the volume (~1.0 ml) collected of the top phase.

$m_{(T\_IS\_S)}$ = Mass of test tube, IS and sample after evaporation described in 3.2.2.

To find the mass of IL in the top phase, the same formula described for the mass of LA in the same phase is used (***Equation 5***).

As the volume collected = 1.0 ml $C_{IL\ (Coll)}$ = 33.72 mg/ml

$m_{IL\ (Top)}$ = 33.72 mg/ml x 1.9 ml = 64.07 mg

Using ***Equation 2***, the volumes of LA and IL in the top phase are found.

$$V_{IL(Top)} = \frac{64.07\,\text{mg}}{895\,\text{mg/ml}} = 0.07159\,\text{ml}$$

$$V_{LA(Top)} = \frac{0.67\,\text{mg}}{890\,\text{mg/ml}} = 0.00072\,\text{ml}$$

Subsequently, the volume of HX is found using the following equation:

Equation 8

$$\boxed{V_{(Top\_T)} - \left(V_{LA(Top)} + V_{IL(Top)}\right) = V_{HX(Top)}}$$

$V_{HX\ (Top)}$ = 1.9 ml – (0.07159 ml + 0.00072 ml) = 1.828 ml

The mass of HX can then be found using ***Equation 2***:

$m_{HX\ (Top)}$ = 655 mg/ml x 1.828 ml = 1197.34 mg

Bottom phase:

To find the masses of the components in the bottom phase, the following equation is used:

Equation 9

$$m_{(Bottom)} = m_{(Total)} - m_{(Top)}$$

$m_{HX\ (Bottom)}$ = 2590.47 mg – 1197.34 mg = 1393.13 mg

$m_{LA\ (Bottom)}$ = 40.12 mg – 0.65 mg = 39.46 mg

$m_{IL\ (Bottom)}$ = 890.2 mg – 64.07 mg = 826.13 mg

Addition of LA + HX:

Continuing with the same example described for Series #2 (Table 3-3), 1.0 ml from a concentration made of 20.28 mg/ml LA/HX was added to the test tube, and the experiment was repeated.

However, to calculate the initial mix, the following equation was used.

Equation 10

$$m_{(Total)} = m_{(Bottom)} + m_{(Added)} + m_{(Top)} - \left(m_{(Coll)}\right)$$

Where:

$m_{(Added)}$ = The mass of the component added.

$m_{(Coll)}$ = The collected mass from the previous run.

$m_{LA\ (Total)}$ = 39.46 mg + 20.28 mg + 0.65 mg – (0.35 mg) = 60.04 mg

Using ***Equation 2***:

$$V_{LA(Total)} = \frac{60.04\,\text{mg}}{890\,\text{mg/ml}} = 0.0675\,\text{ml}$$

To find the mass of HX added, the following equation is used:

Equation 11

$$m_{HX(Added)} = 1\,\text{ml}_{(\text{Clean HX})} \times \rho_{HX} + \left(1\,\text{ml}_{(\text{HX}+\text{LA})} - \frac{m_{LA(Added)}}{\rho_{LA}}\right) \times \rho_{HX}$$

$$m_{HX(Added)} = 1\text{ml} \times 655\text{mg/ml} + \left(1\text{ml} - \frac{20.28\text{mg}}{890\text{mg/ml}}\right) \times 655\text{mg/ml}$$

$m_{HX\ (Added)}$ = 1295.07 mg

Using ***Equation 10*** the total mass of HX can be found.

$m_{HX\ (Total)}$ =1393.39 mg + 1295.07 mg + 1197.08 mg – (630.04 mg)

$m_{HX\ (Total)}$ = 3255.51 mg

Equation 10 is also applied to find the total mass of IL:

$m_{IL\ (Total)}$ = 826.13 mg + 0 mg + 64.07 mg – 33.72 mg

$m_{IL\ (Total)}$ = 856.48 mg

The top and bottom phases are then calculated as previously shown in the example.

The mass fractions are calculated for each part *"j"* (mix, top or bottom) in equation:

Equation 12

$$\widehat{x}_{ij} = \frac{m_{ij}}{\sum_{i:LA,IL,HX} m_{ij}}$$

The corresponding mole fractions are calculated from equation:

Equation 13

$$x_{ij} = \frac{n_{ij}}{\sum_{i:LA,IL,HX} n_{ij}} \qquad n_{ij} = \frac{m_{ij}}{Mw_i}$$

3.4 Sources of error

Excel solver was used to minimize the difference between the calculated and measured concentrations by incorporating an additive error term in the calculations representing the potential error in the volumes added or removed. For the experimental

Series #2, a possible error in adding 1 ml of pure HX or 1 ml of LA/HX was used with each of the adding steps. However, the value was allowed to be either positive or negative, in the range - 0.06 to + 0.06 ml, given that the volumes were adjusted by eye to the total volume line desired in the centrifuge tube, and the lines were about 1 mm apart in the straight section of the tube, graded for 0.1 ml volume resolution. The collection error was also allowed to vary between - 0.06 and + 0.06. These values were assumed to be average errors, and it was considered that they might differ for each replicate, since the operation was done sequentially for the test tubes 1, 2 and 3.

CHAPTER 4 RESULTS AND DISCUSSION

4.1 Preliminary experiments

To select an appropriate solvent, it was necessary to decide between chloroform, of which no information on miscibility or reaction with IL was available, and HX which has been used previously in other studies involving this particular IL. A triphasic mixture resulted from the addition of water, chloroform and IL (Figure 4-1). However, chloroform formed a bottom layer, below the water phase, due to its greater density (Matyash et al., 2008). Using chloroform as the solvent would not be as beneficial as having the interface set between the IL and the solvent, allowing the LA to partition readily if needed in future experiments. Compared to HX which forms a phase above the IL and has direct contact to allow LA or any product for that matter to partition, chloroform was deemed unsuitable.

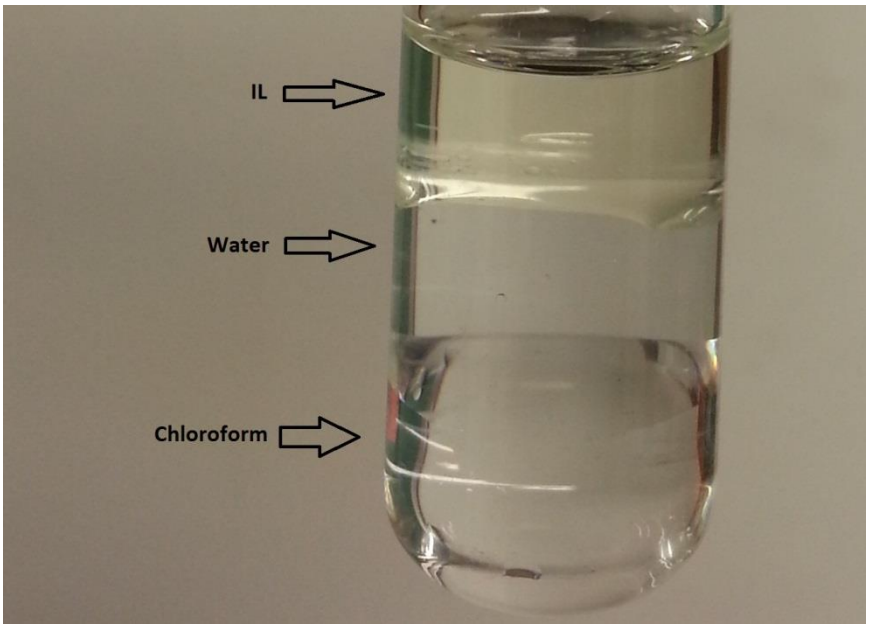

Figure 4-1: A triphasic mixture of 1 ml dH_2O, 1 ml IL and 1 ml chloroform. The photograph was taken after equilibration by vortexing and centrifugation.

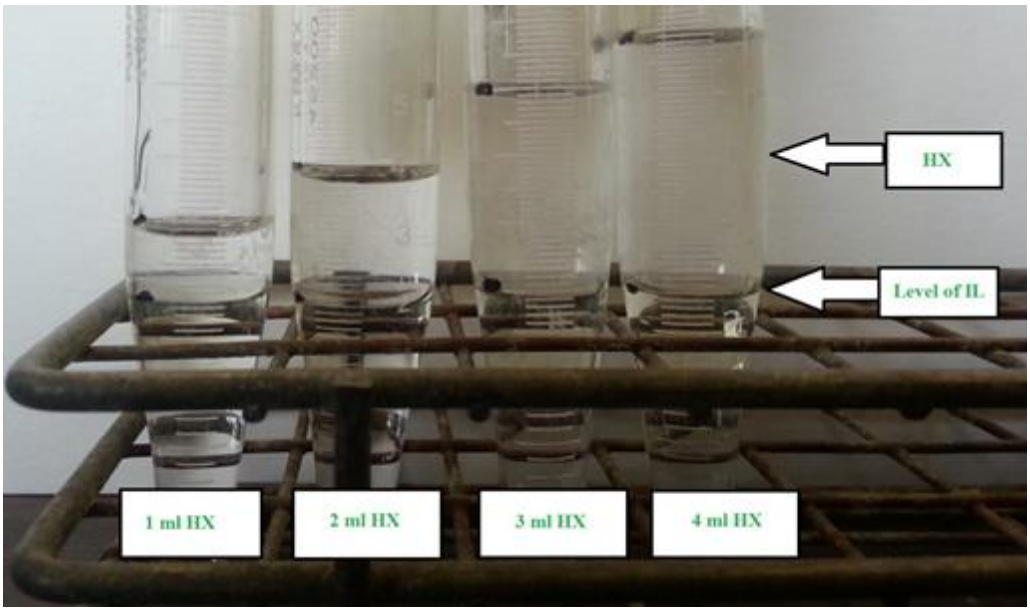

Figure 4-2: Four different volumes of HX added to four separate graduated centrifuge conical bottom test tubes containing 1.0 ml dH_2O and 1.0 ml IL (volume of HX indicated at the bottom of each individual tube). The volume level of the IL phase and the HX phase is indicated by the arrow. The photograph shown here was taken before the tubes were vortexed and centrifuged.

The HX added to each test tube did not show any indication of miscibility (Figure 4-2) before allowing equilibration by vortexing and centrifugation. All test tubes indicated a triphasic system. After vortexing and reaching equilibrium, the miscibility between IL and HX was evidenced by the change in the position of the interface. The first test tube that had a single ml of HX added to the system made only two phases: water and IL up to the 3.0 ml mark (Figure 4-3). The additions of 2.0, 3.0 and 4.0 ml HX showed an increase of 1.5 ml in the IL phase, from 2.0 ml to 3.5 ml. After leaving the samples for 24 hrs, no change in the phases were visible. Hence, the IL phase was saturated with HX in all three tubes. To be sure of the volume of HX taken up into the IL phase, the triplicate experiment of 1.0 ml IL, 1.0 ml dH_2O and 4.0 ml of HX all showed an increase of 1.5 ml in the IL phase after being vortexed and centrifuged. This preliminary experiment was also

important in determining the volume of HX that would be sufficient to distinguish a top and bottom phase in the following experiments.

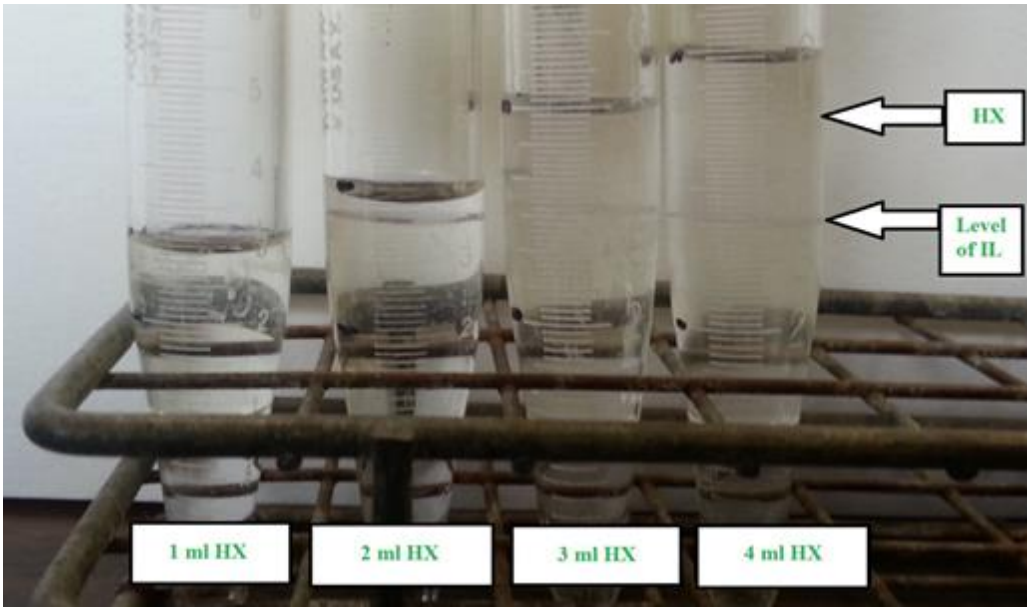

Figure 4-3: Four different volumes of HX added to four separate graduated centrifuge conical bottom test tubes containing 1.0 ml IL and 1.0 ml dH_2O. Each test tube was equilibrated by vortexing and centrifugation.

4.2 LA effect

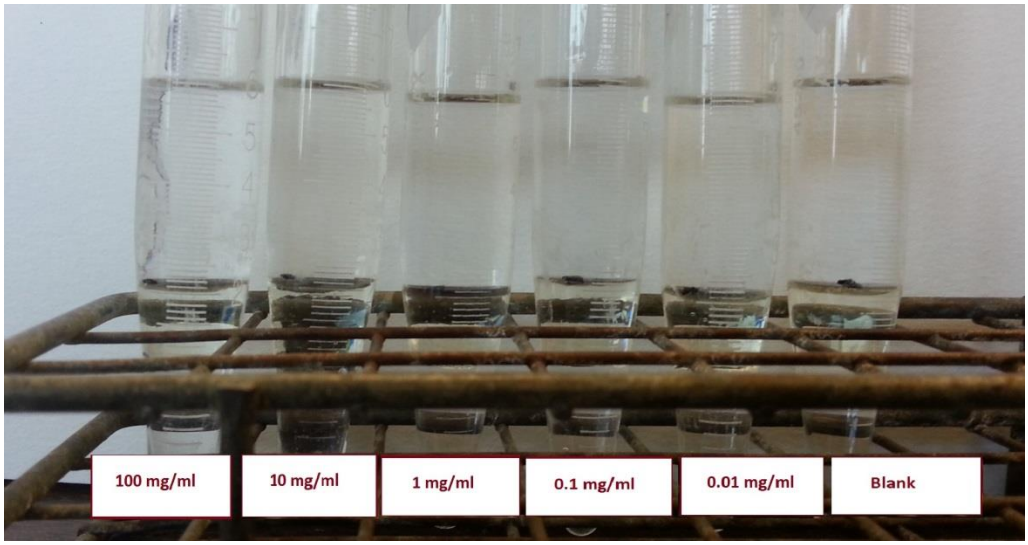

Figure 4-4: Five different concentrations LA in HX (labeled beneath each test tube) added to separate test tubes containing 1.0 ml dH_2O and 1.0 ml IL. 4.0 ml of the LA in HX concentrations was added to each while the sixth test tube acted as a blank with no concentration of LA in HX. This photograph was taken before equilibration by vortexing and centrifugation. The black marker serves to show the interface level of IL and HX.

To determine the effect, if any, that LA would have on the biphasic system of IL (bottom phase) and HX (top phase), 4.0 ml of different concentrations of LA in HX were added to 1.0 ml dH_2O and 1.0 ml IL (Figure 4-4). As noted earlier, water was always present as a separate phase at the bottom but the focus here with the addition of LA was on the IL (bottom) and HX (top) phases. After equilibration, all test tubes showed no change in volume at the interface between the IL and water (Figure 4-5). The blank test tube, as well as the test tubes with concentrations of LA/HX from 0.01 mg/ml - 1 mg/ml, showed the same volumetric increase of 1.5 ml seen in Figure 4-3 of the IL phase into the top HX phase (or vice versa) and can be attributed to the miscibility between HX and IL. However, a single phase was visibly shared by the HX and IL in the test tube containing 100 mg/ml LA/HX. The concentration of 10 mg/ml showed an increase of 2.1 ml in the volume of IL

phase. No changes were observed after 24 hrs. This experiment helped highlight a region of interest where the addition of LA had a direct effect on the different phases. Additional tests with 9, 8 and 7 mg/ml LA in HX solutions provided a sense of the change in volume expected, as indicated in Figure 4-6.

Figure 4-5: Five different concentrations LA in HX (labeled beneath each test tube) added to separate test tubes containing 1.0 ml dH_2O and 1.0 ml IL, shown after equilibration by vortexing and centrifugation. The three black marks on each test tube serve to show the level of IL before (middle mark) and after equilibration (top mark). The bottom marks show the interface between the IL and water.

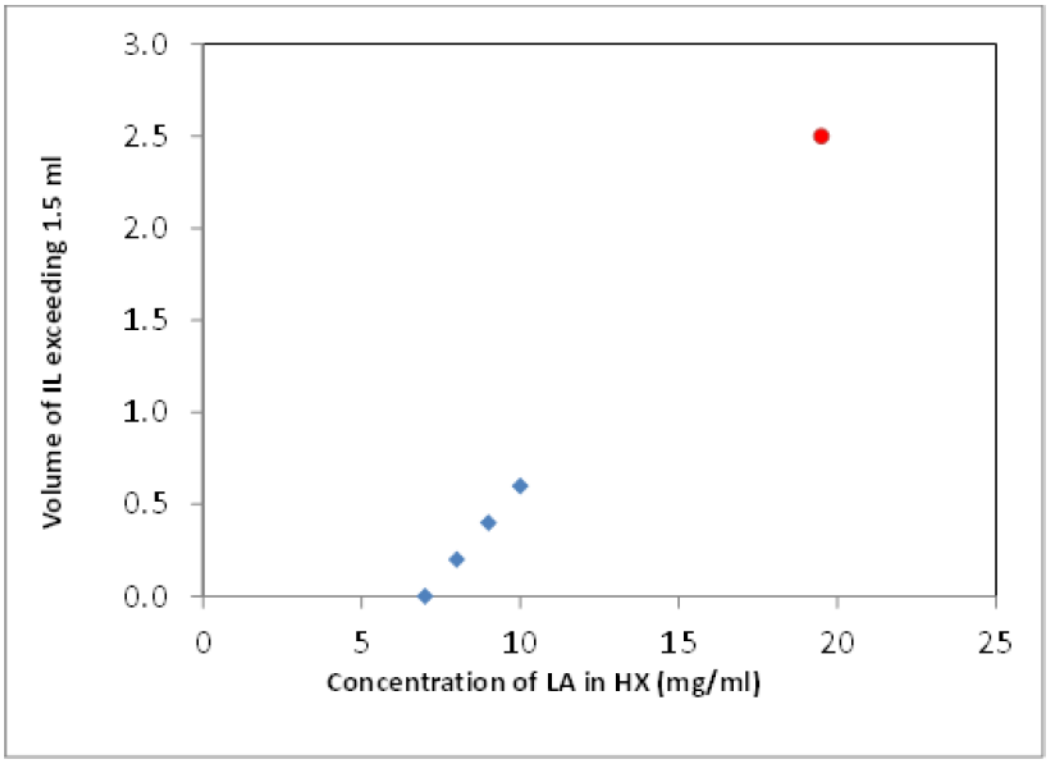

Figure 4-6: Increase of IL phase volume beyond 1.5 ml into the HX phase due to LA. The graph is representative of concentrations of LA in HX volumes of 4.0 ml. The blue points denote experimental values whereas the red point is an extrapolation showing the critical level in which IL and HX would become a single phase.

A final preliminary experiment was carried out to test whether FAME of LA was so volatile that evaporating the sample solvent to dryness under a stream of nitrogen might cause significant losses of the FAME (3.2.1.4). The mean loss of LA FAME after evaporation was found to be only 0.8%. Due to the negligible loss, the possibility was not accounted for in the results.

4.3 Phase diagrams

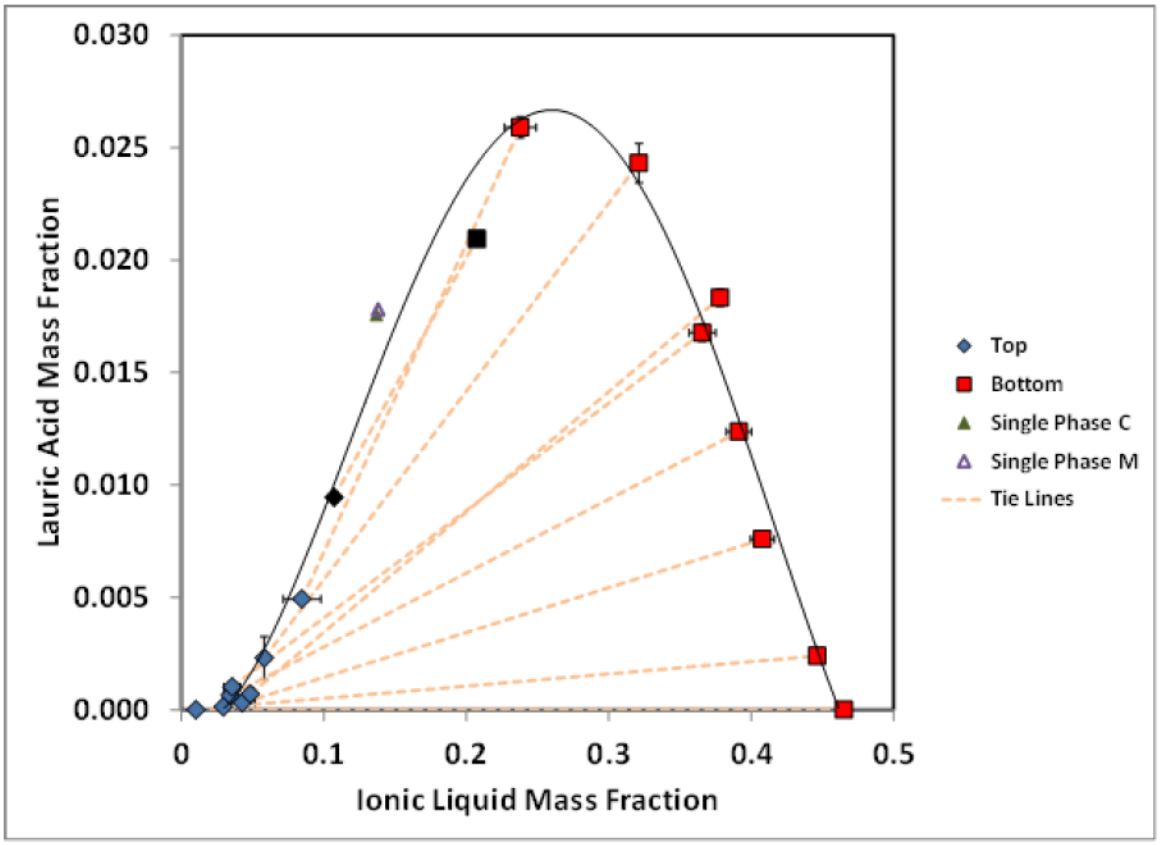

Figure 4-7: Mass fraction phase diagram of LA+IL+ HX with experimental tie lines between the top (HX rich) and bottom phases (IL rich). The experimental points are taken from the collected data resulting from Series #1 and Series #2 illustrated in Table 3.2 and Table 3.3.

After the determination of the compositions of both phases as described in the methods section, the values were plotted in a Cartesian graph, rather than a triangular plot, given the small values of the LA mass fractions. The top and bottom points are means of triplicates except for the points highlighted in black, which are outliers. All points include the corrections for sources of error (Table 4.1). Each error bar represents the standard deviation from the average mass fraction. The mass fraction of HX can be found by subtracting from 1 the sum of any x and y coordinates for a point in Figure 4-7. The experimental equilibrium tie lines linking the top and bottom phases allow the

determination of both IL and LA mass fractions anywhere on the line and consequentially the mass fraction of HX. A polynomial trend line of the fourth order is included to guide the eye. Approximately any point beyond the boundary trend line (a point outside the curve of the top and bottom tie lines) would constitute a monophasic system rather than a biphasic one (i.e., in reality monophasic = two phases where IL + HX is one phase and water the other, biphasic = three separate phases of IL, HX and water). "Single Phase C" is a theoretical point comprised of all the calculated additions from Series #2 in Table 3-3 as described in the example outlined in section 3.3. The point represents a monophasic system where both IL and HX are visibly a single phase. "Single Phase M" is the measured point of all the additions from Series #2 that resulted in a single phase. A photograph of the final addition in Series #2 of which the single phase was measured is shown (Figure 4-8), illustrating the absence of an interface between the IL and HX phases.

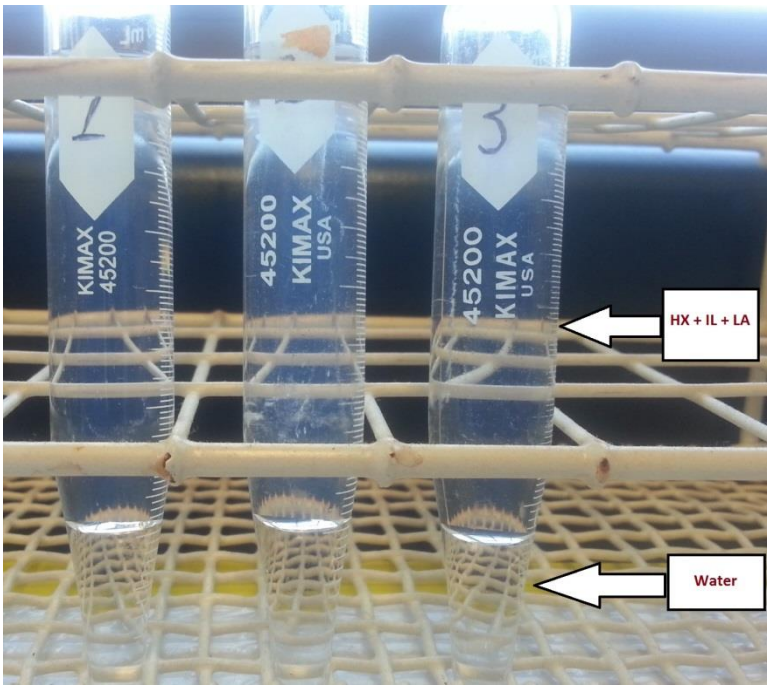

Figure 4-8: Triplicate experiment from Series #2 with the final addition of LA and HX (100 mg LA and 7.0 ml HX total added to 1.0 ml IL and dH_2O). The top (HX) and bottom (IL) phases are not visible. The photograph was taken after equilibration by vortexing and centrifugation.

The average mass values for the "Single Phase C" point did not initially correspond to the measured "Single Phase M" values at the end of Series #2 (Table 3-3). In order to explain such a difference in value, several possible experimental errors listed below were added to the computations for each run in Series #2:

1) The amount of HX and LA added in each series, initially and after every addition, might not have been exact.

2) Variability in the 1.0 ml HX added back to the system to replenish the 1.0 ml extracted in each run.

3) Error in the 1.0 ml collected from the top phase during each run.

The maximum error in all cases was set to ± 0.06 ml because the divisions on the test tubes were 0.1 ml. Another error that was explored was the possibility of incorrectly reading the

volume of IL phase in the graduated test tube. When this error was allowed to increase up to a maximum of ± 0.3 ml, there was minimal change in the masses observed; therefore this possible source of error was discarded.

Table 4-1: Percentage of difference in mass from the final calculated Single Phase C point and the final mass measured, Single Phase M point from Series #2. The percentages are shown before and after including the possible sources of error.

% Before error incl.	**IL**	**LA**	**HX**	**% After error incl.**	**IL**	**LA**	**HX**
#1	14.1	8.4	-4.4	**#1**	6.8	0.2	2.5
#2	2.4	6.5	-2.4	**#2**	-2.8	-1.2	4.4
#3	-4.1	4.9	-2.1	**#3**	-7.4	-0.8	2.7

By adding the possible sources of error, the percentage of difference in mass from the final calculated single phase to the measured single phase was decreased, indicating that the possible sources of error are legitimate (Table 4-1). Only the collection error for the first run of the triplicate reached the maximum boundary of + 0.06, while all the others were within the range (Table 4-2). All the average errors were positive. There seems to be a bias in the estimation of the level, possibly due to repeatedly underestimating the actual volume added or removed. Since the calculated and measured compositions found agreement with the 'addition' of such small biases, which are within the reasonably estimated experimental error, it is likely that such biases did exist, and were on average, of the magnitudes calculated.

Table 4-2: Values of the systematic addition and collection errors in Series #2.

Addition error		**Collection error**	
#1	0.017	**#1**	0.060
#2	0.032	**#2**	0.059
#3	0.028	**#3**	0.043

As all three sources of error helped decrease the percentage of error (possible error in the collected 1.0 ml decreased the percentage more than the possible error in either additions), precautionary steps should be taken in future experiments, by being more precise in the additions of the mixtures and more importantly, extracting a precise volume. Suggestions to reduce the errors are included in Chapter 5. All the figures within this Thesis include the sources of error calculated for the masses in Series #2 (Table 4-1). The values used to construct the phase diagram in Figure 4-7 are included in Table 4.3. The non-averaged mass fractions for the top, bottom, mix points and the measured single phase points as well as the original experimental mass fraction values without the corrections for possible errors are included in Appendix C.

Table 4-3 : Mass fraction experimental tie lines within the biphasic region for the system LA + IL + HX.

Top phase (HX rich)			**Lower phase (IL rich)**		
LA	**IL**	**HX**	**LA**	**IL**	**HX**
0.0001	0.0297	0.9701	0.0024	0.4465	0.5511
0.0003	0.0428	0.9569	0.0076	0.4079	0.5845
0.0007	0.0345	0.9648	0.0124	0.3914	0.5962
0.0010	0.0357	0.9633	0.0168	0.3657	0.6175
0.0007	0.0484	0.9509	0.0183	0.3782	0.6034
0.0023	0.0582	0.9395	0.0243	0.3212	0.6545
0.0049	0.0847	0.9104	0.0259	0.2379	0.7362
0.0095	0.1071	0.8834	0.0209	0.2074	0.7716
0	0.0104	0.9896	0	0.4652	0.5348
Single phase M	Single phase M	Single phase M	0.0178	0.1382	0.8440
Single phase C	Single phase C	Single phase C	0.0176	0.1369	0.8455

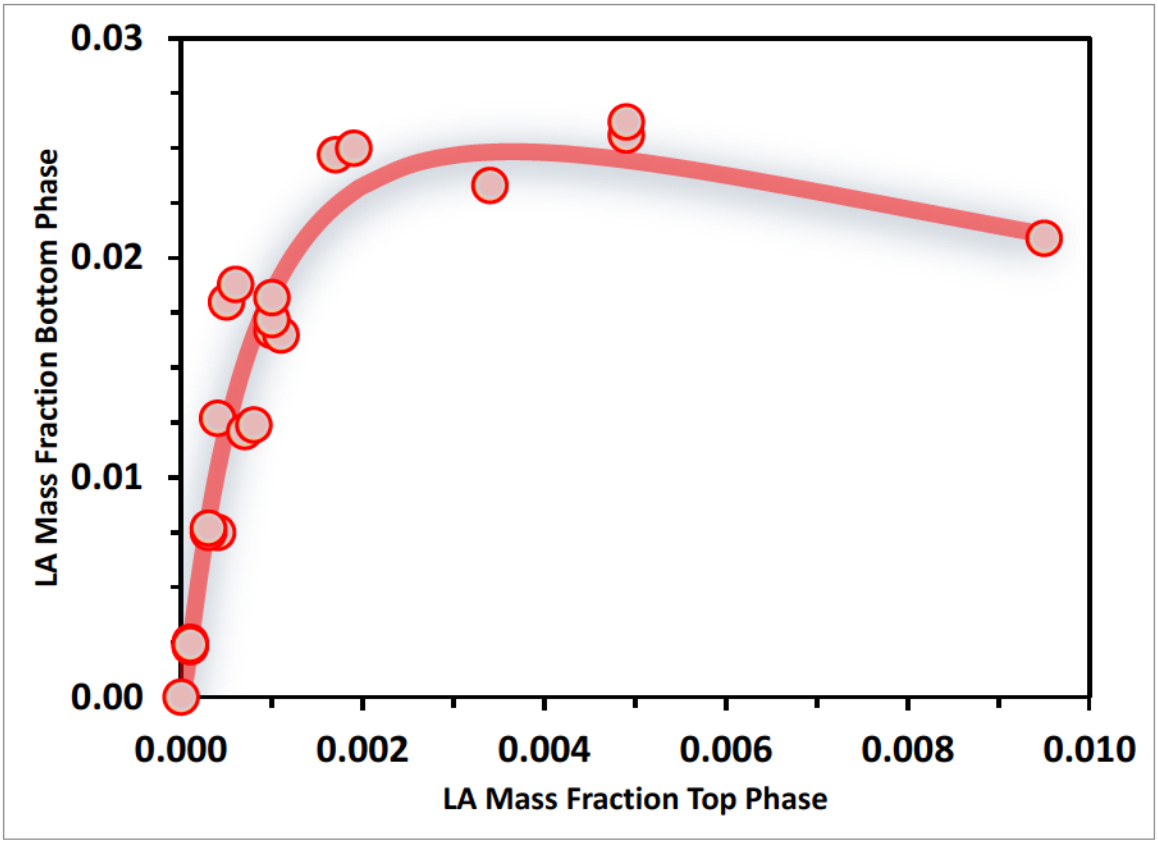

Figure 4-9: Mass fractions of all the experimental points for LA in the top and bottom phases.

The polynomial trend line in Figure 4-9 helps approximate the composition of LA in either top or bottom phase if one of the two is known. It therefore represents the equilibrium tie lines.

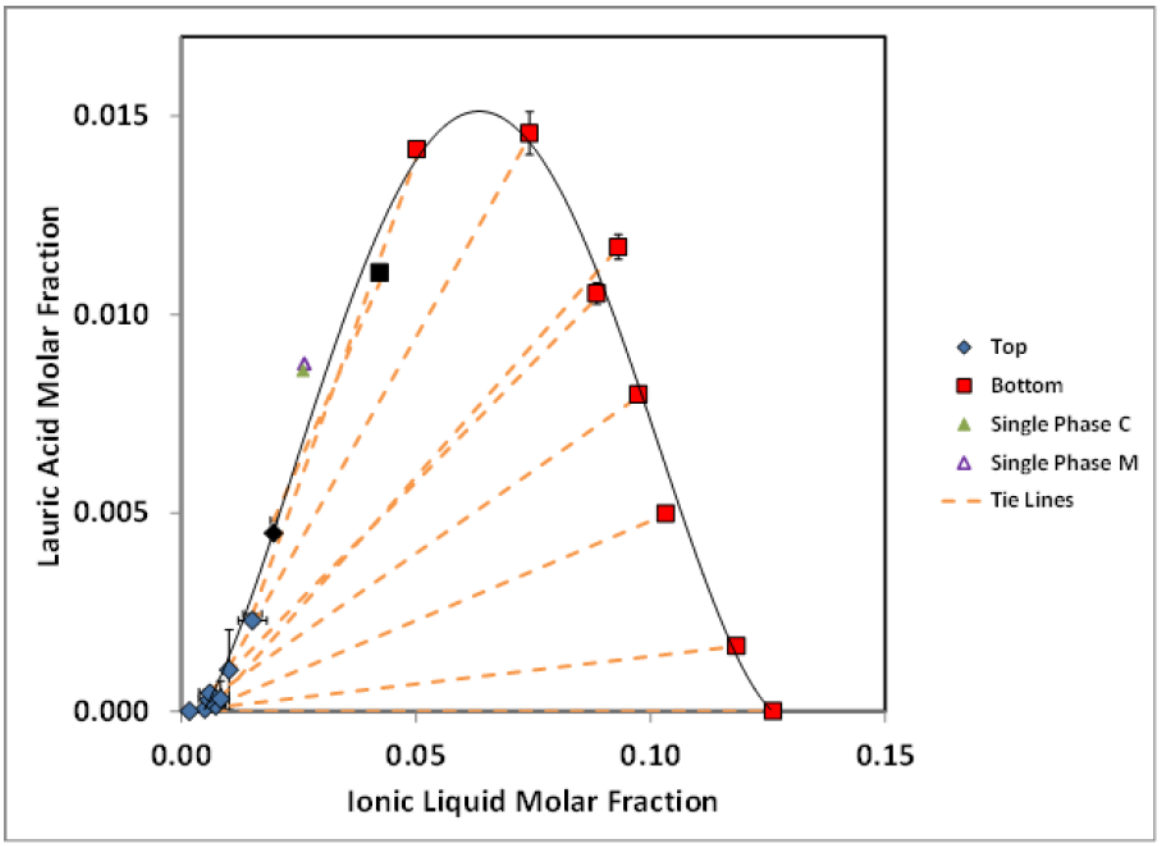

Figure 4-10: Molar fraction phase diagram of LA+IL+HX from the same experimental data used to find the mass fractions in Figure 4-7. Each error bar represents the magnitude in error from the standard deviation.

A similar trend to that of the data in mass fraction (Figure 4-7) is observed after converting the data to molar fraction (Figure 4-10). As above, the tie lines show the equilibrium points between the bottom phase and the corresponding point in the top phase (Table 4-4). The trend line denotes an approximation at which any point beyond the line would constitute a monophasic system (i.e. in reality IL + HX as a single phase and water at the bottom) whereas any point within the line and experimental points would represent a biphasic system (i.e. in reality three separate phases of IL, HX and water).

Table 4-4: Molar fraction experimental tie lines within the biphasic region for the system LA + IL + HX.

Top phase (HX rich)			**Lower phase (IL rich)**		
LA	**IL**	**HX**	**LA**	**IL**	**HX**
6.0E-05	0.0051	0.9949	0.0016	0.1183	0.8800
0.0001	0.0074	0.9925	0.005	0.1033	0.8917
0.0003	0.0059	0.9938	0.008	0.0974	0.8946
0.0005	0.0061	0.9934	0.0105	0.0885	0.9009
0.0003	0.0084	0.9913	0.0117	0.0931	0.8952
0.0010	0.0102	0.9888	0.0146	0.0742	0.9112
0.0023	0.0152	0.9825	0.0142	0.0502	0.9357
0.0045	0.0196	0.9759	0.0111	0.0422	0.9467
0	0.0017	0.9983	0	0.1261	0.8739
Single phase M	Single phase M	Single phase M	0.0088	0.0262	0.9650
Single phase C	Single phase C	Single phase C	0.0086	0.0259	0.9654

The molar fraction value for IL in the blank run (0.126) is approximately twice as large as the value (0.053) found in the reported literature (Makowska et al., 2010), indicating that HX is less soluble in the IL than what is reported. This discrepancy could be a result of the addition of water in the experiments conducted here, whereas the procedure followed by Makowska et al. (2010) did not include an aqueous phase. As reported earlier in the literature review, water is used to separate hydrocarbons from the IL (Earle et al., 2003). The studies by Anderson et al. (2009) and Lago et al. (2012) that showed less miscibility of the alkanes dodecane and nonane with IL when water was added to the system confirm our results of decreased miscibility of HX with IL when compared to the results of

Makowska et al. (2010). As with the mass fraction for LA in the system, the polynomial trend line in Figure 4-11 helps approximate the mole fraction of LA in either top or bottom phase if one of the two is known.

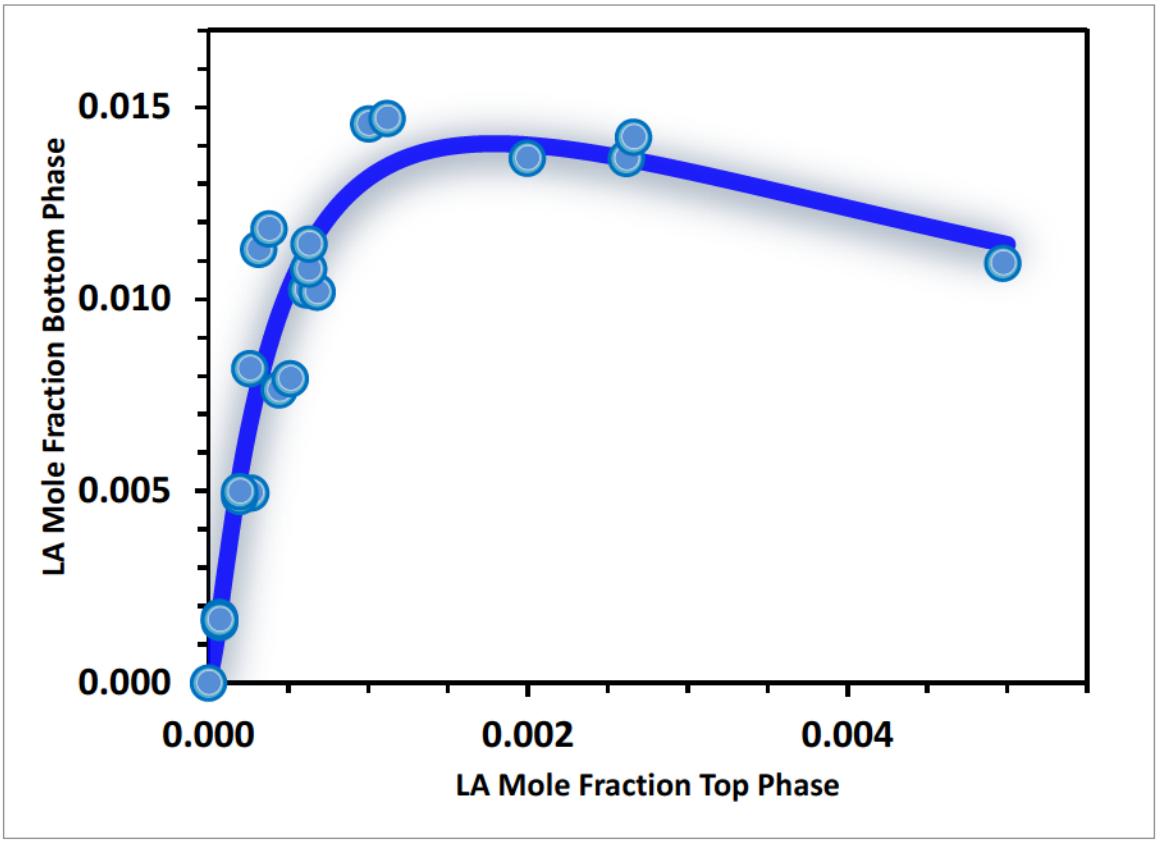

Figure 4-11: Molar fractions of all the experimental points for LA in the top and bottom phases.

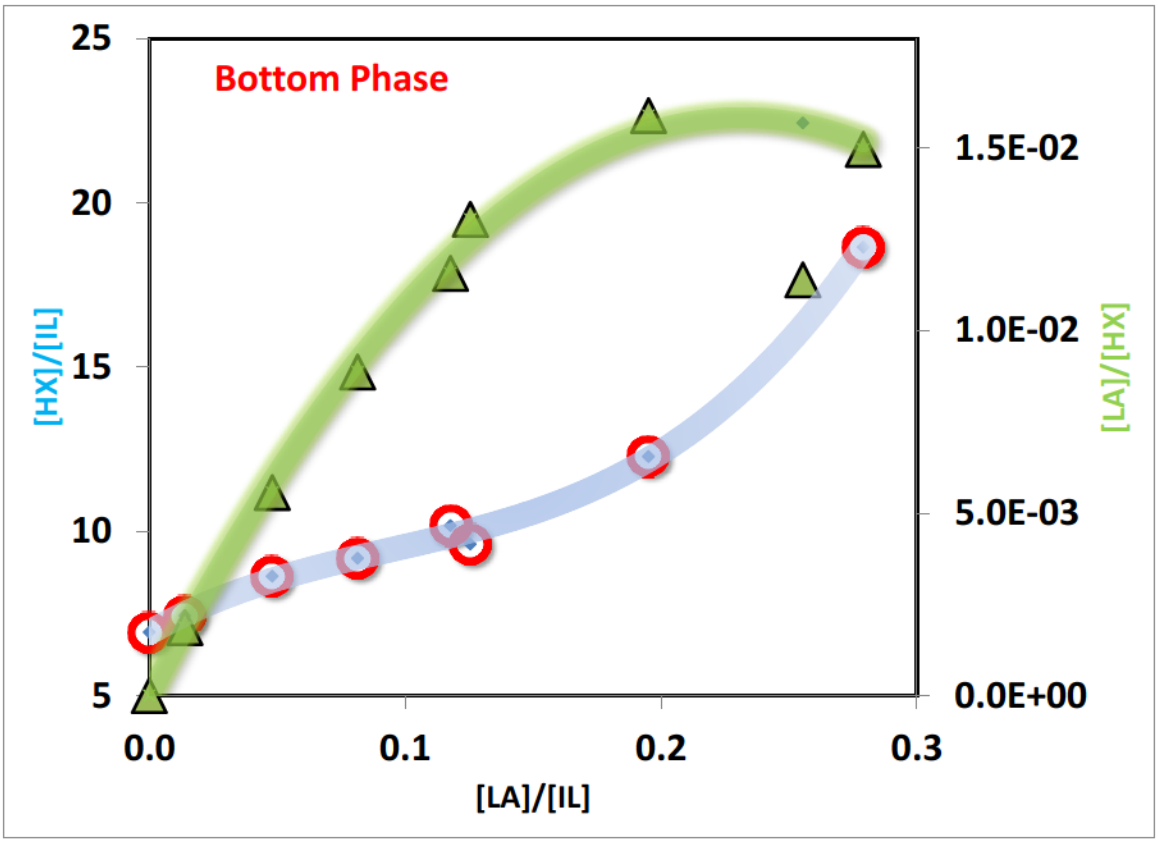

Figure 4-12: Molar ratios of [LA]/[IL], [HX]/[IL] and [LA]/[HX] in the bottom phase. The blue curve highlights the relationship between the ratios of [HX]/[IL] and the ratios of [LA]/[IL], whereas the green curve approximates the molar ratios of [LA]/[HX] and their relationship with [LA]/[IL].

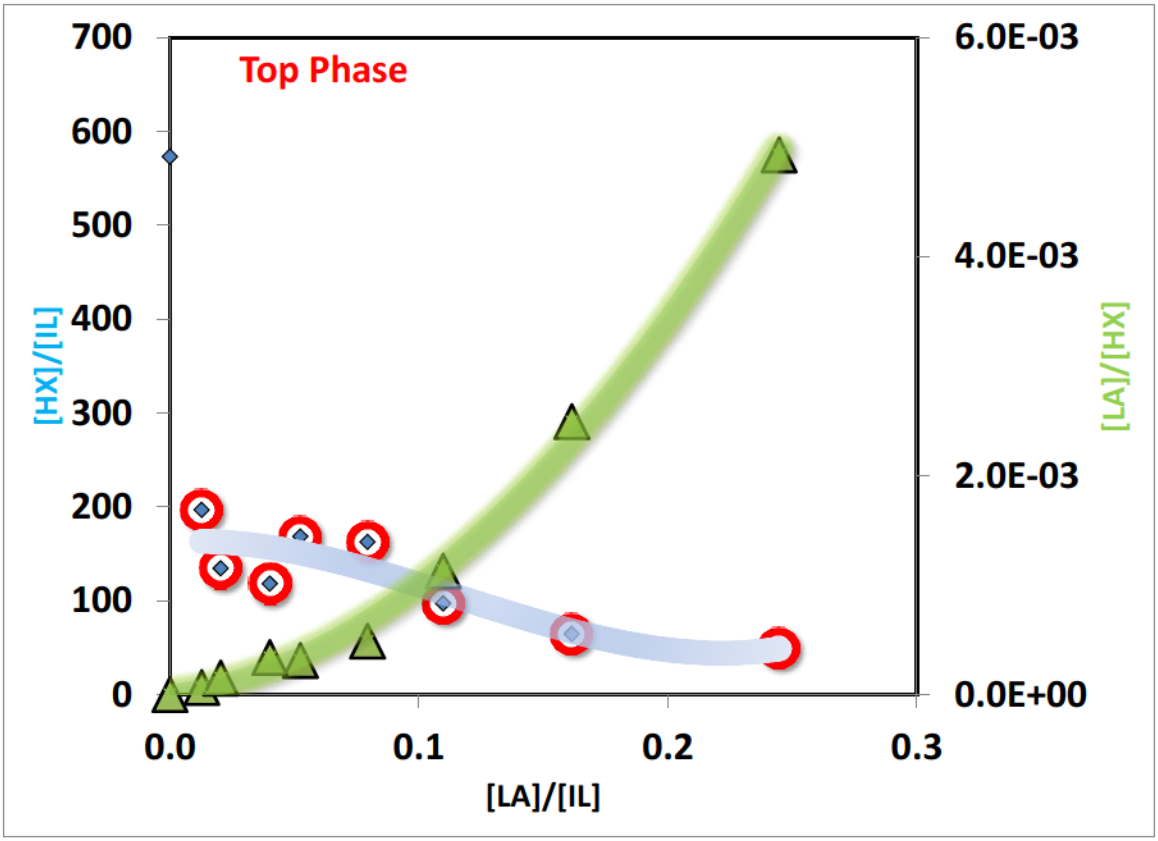

Figure 4-13: Molar ratios of [LA]/[IL], [HX]/[IL] and [LA]/[HX] in the top phase. The blue curve highlights the relationship between the ratios of [LA]/[IL] and the ratios of [HX]/[IL], whereas the green curve approximates the molar ratios of [LA]/[HX] and their relationship with [LA]/[IL]. Note the blank sample on the [HX]/[IL] axis corresponding to approximately 573 when LA= 0.

From the molar fractions it was possible to derive molar ratios in each phase, as shown in the graphs. The [LA]/[IL] concentration has similar values in both the top (Figure 4-13) and bottom phases (Figure 4-12), as seen by the extent of the scales in both x-axes. The ratios of molar concentrations of LA to IL in both the bottom and top (Figure 4-14) suggests a proportional interaction for both molecules in both phases. A speculation can be made that LA acts to solubilize IL in HX and HX in IL.

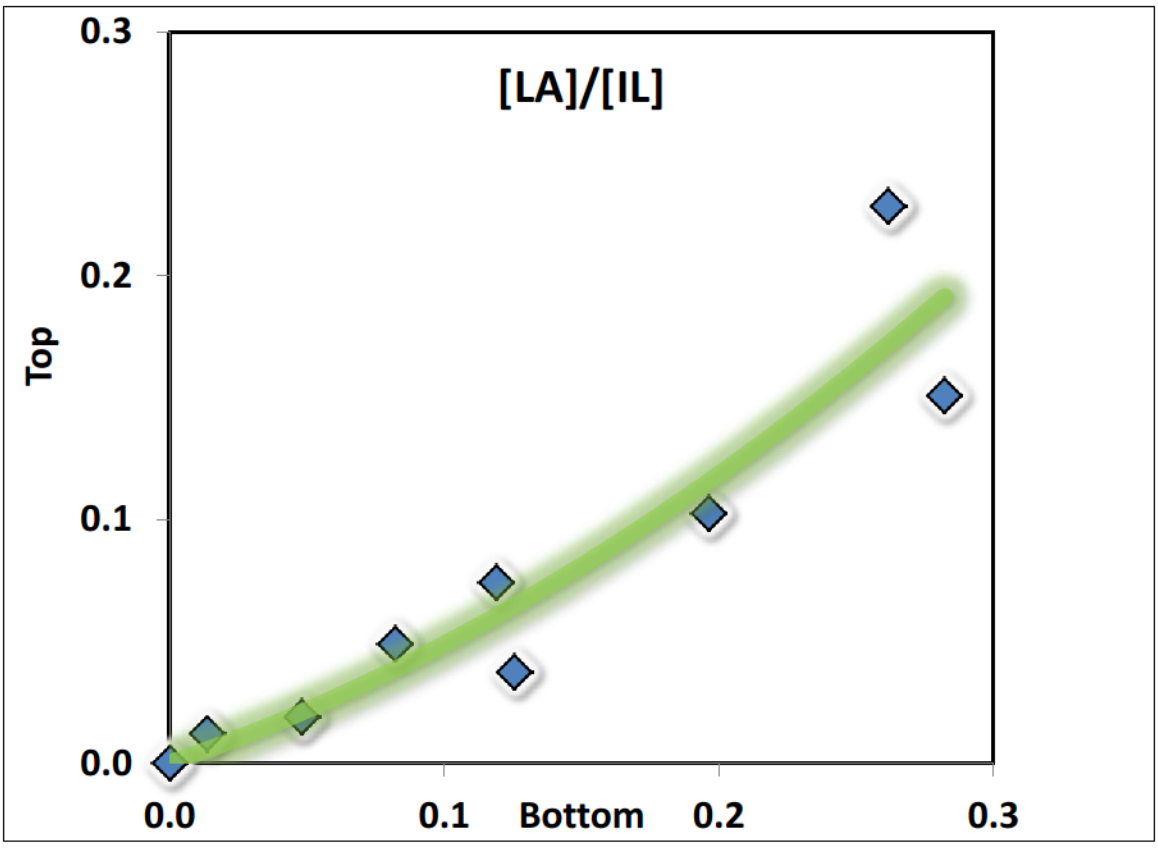

Figure 4-14: Molar fraction ratio of [LA]/[IL] in the bottom phase (x-axis) and top phase (y-axis).

To suggest a possible explanation for this behaviour, one can consider the two types of intermolecular forces probable between IL and LA. The first one is via weak van der Waals interactions between the aliphatic chains of both molecules. The second one is associated with the very strong polar attraction between the electron-rich carboxylic group of the LA and the positively charged phosphonium of the IL (Figure 4-15), leading to the formation of a complex. The complex would have a reduced overall polarity, compared to the separate molecules. Therefore the aliphatic chains of the LA+ IL complex will enhance the van der Waals interaction with other LA molecules, and would increase the compatibility with the nonpolar HX molecules as well. This provides a

reasonable qualitative explanation for the presence of similar molecular ratios [LA]/[IL] in both phases, and for the increase of this ratio and the changes of [HX]/[IL] ratios as the concentration of LA in the system increases.

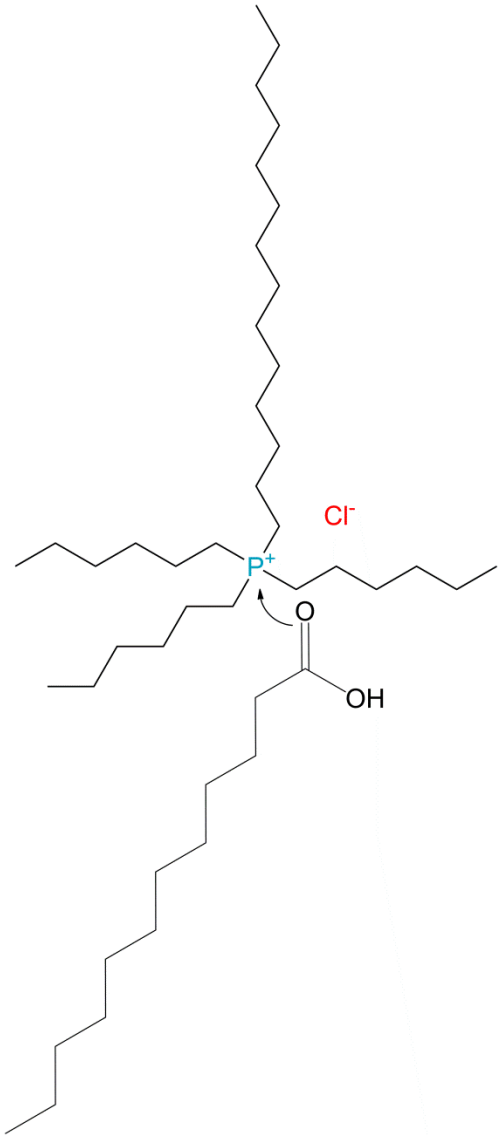

Figure 4-15: Schematic depiction of the proposed possible interactions between IL and LA.

The effect of adding FFA in such systems should therefore be accounted for in terms of their solubilizing effect on the IL with the solvent. Figure 4-5 and Figure 4-8 show the tremendous solubilizing effect a FFA has, whereby a large concentration of LA in HX

was added to IL and resulted in a single phase. Yet if the same amount of HX was added to the IL without LA, the only change in volume would be 1.5 ml as a result of the miscibility between the two liquids. Because ILs have been gathering much attention as mediums for possible oil extractions, understanding and quantifying the solubilizing effect of the particular oil used should help to achieve full extractions of the product.

These results can be extrapolated to predict how other molecules of different polarity might behave in this system. For instance, any groups of molecules that increase the polarity of the FFA would have a higher tendency to remain in the IL. On the other hand, if a FFA with an aliphatic chain length longer than LA was to be added to the system of IL and HX, the lower polarity of the FFA would result in a higher affinity towards the nonpolar HX phase.

A similar system of LA, IL and HX exposed to higher temperatures may yield different results as two forces would act to counter each other. At higher temperatures, the solubility of IL with the alkane HX would increase as shown in previous studies by Makowska et al.(2010), and Anderson et al (2009). However, the solubilizing effect of LA on the IL would decrease due to the decrease in van der Waals forces at higher temperatures and thus a higher concentration of LA would partition into HX than in the IL phase. The two opposing forces need to be quantified experimentally to determine the effect on the two phases and LA, as one force might be larger than the other.

4.4 Potential applications

The original aim of this study was done to determine if HX is suitable to extract FFA, a product of hydrolysis, from the IL. The results of the phase diagrams show that LA remains mainly within the IL, displaying a higher affinity to the IL over HX. The results

also showed a threshold concentration of LA beyond which the biphasic mixture of the IL and HX became a single phase due to the solubilizing effect of the LA. This in turn makes it difficult to extract product from the proposed hydrolysis reaction in IL with HX. The phase diagrams also suggest that the tendency of a component to stay in the IL phase increases with its polarity. Thus, the order of solubility in the IL decreases from: FFA→MAG→DAG→TAG, whereas the inverse would be true in HX. This acts as a probable confirmation to the second possibility proposed in the introduction that the IL is in fact a capable supportive medium for free enzymes and corresponding reactions, and the limited recovery of FFA is due to the failure of HX to extract all the FFA produced from hydrolysis.

Referring back to the results of the TLC plate from the hydrolysis reactions of canola oil in the IL (Figure 1-2), bands of TAG were clearly visible whereas the bands of FFA were very faint. This confirms the effect of polarity on the solubility of TAG and FFA from the IL to HX. In conjunction with the experimental phase diagrams that act as supporting evidence, the faint bands of FFA on the TLC plate point towards a high likelihood that a hydrolysis reaction did indeed occur in the IL. The phase diagrams constructed showed that the amount of LA in HX after reaching equilibrium and at different concentrations were markedly low in comparison to the amounts of LA in the IL. In comparison, the HX added on top of the IL that acted as a medium for the hydrolysis reaction was only allowed to settle for 10 minutes without vortexing, yet FFA, a product of hydrolysis was still observed. However, it should be noted that the FFA produced from the hydrolysis of the canola oil (mainly oleic and linoleic acids) are less polar than LA due to their longer hydrocarbon chains, and as a result, would be more drawn towards the HX layer. Although

the amount of FFA extracted was visibly low, [P_{66614}] [Cl] can be considered as a potential IL medium for hydrolysis reactions but a more efficient method of extracting the FFA should be determined first.

CHAPTER 5 CONCLUSIONS AND FUTURE WORK

Summing up, the concentration range in which LA visibly affects the solubility of IL with HX was determined through several preliminary experiments. Experiments were then conducted within that range to help construct phase diagrams of the FA, IL and HX. In both mass and molar fraction phase diagrams, a trend line was added to help approximate the boundary between monophasic and biphasic systems. Tie lines between the two phases were calculated.

The biphasic zone is present for LA mole fractions smaller than 0.015 in the IL layer and up to 0.005 in the HX layer. The mole fraction of IL in the phases is below 0.02 in the HX layer, and up to 0.12 in the IL layer. The single phase is around a mole fraction of 0.03 for IL and 0.01 for LA.

The molar ratios of LA/IL in the top and bottom phases show that the ratio of IL molecules per LA molecule in both the top and bottom phases is similar. This discovery suggested a possible mechanism through which the LA promotes solubilization of the IL in HX and vice versa. This also suggests that a comprehensive study on the possible mechanisms of interactions between LA, IL and HX is warranted. Using proton NMR spectroscopy of the IL phase in conjunction with the phase diagrams (Nicotera et al., 2005) may help understand how the FA and the solvent interact with IL.

A better definition of the phase diagram requires collecting more experimental points where the IL and HX become a single phase. However, at present it is already possible to predict concentrations in the top or bottom phases that satisfy equilibrium conditions within the range shown in the phase diagrams, and plan experiments accordingly. In hindsight, modifications discovered can be added to the experimental

procedure may improve accuracy and reduce experimental error. A more precise instrument, instead of a Pasteur pipette, should be used for the addition and removal of liquids. This would help reduce the experimental errors described in the results and discussion. Weights should also be noted after every step. The volume of water was kept constant through the experiment, yet the exact weight was not taken. As water is used to separate IL and HX, the molar fraction of water should be taken into account to develop quaternary phase diagrams which may help determine how much of an impact water has on phase and product separation.

Although less polar solvents like nonane or dodecane are not as miscible as HX with IL (Anderson et al., 2009; Lago et al., 2012), they would be less suitable as extracting solvents for FAs precisely because of their low polarity. However, it is possible to employ a more polar solvent than HX such as dichloromethane since it is "borderline" polar and not very soluble in water. By being more polar than HX, there is possibly a better chance that more LA can be extracted. However, as was the case with chloroform, dichloromethane has a higher density than water (1.325 g/ml) which would constitute a bottom layer in a system of IL and water. Thus, dichloromethane might not be suitable as an extracting solvent because the interface of the IL would be with water and the product would not readily partition into dichloromethane. The density of a solvent should therefore be considered so that it be less than the IL to allow the solvent to settle as a top phase, above the IL. The miscibility of the solvent and the IL should also be determined before deciding its suitability as an extracting solvent.

It can be concluded from the phase diagrams that this particular IL would not be particularly suitable for hydrolysis reactions. The majority of the FFA tends to remain in

the IL and extracting the product would be difficult since the FFA favours IL over HX. However, if there is an alternative method to extract the FFA without affecting the IL and the enzymes suspended within, then the IL might become suitable as a medium for enzymatic hydrolysis reactions. As a possible extracting solvent that has been dismissed due to its high density and formation of a layer below water, chloroform might be used to extract products of hydrolysis. A proposed experiment would be to conduct a hydrolysis reaction in IL as outlined in Appendix A. After the reaction is complete, without the addition of 1 ml water, added chloroform would pass through the IL layer and settle at the bottom as a separate layer. As the chloroform goes through the IL, the FFA from the hydrolysis reaction might have a higher attraction to migrate into the chloroform layer due to its partial polarity, more so than the nonpolar HX. The system would not be vortexed so as to retain the enzymes in the IL and not allow the enzymes to partition into the chloroform layer. After a set amount of time the chloroform layer could be extracted by inserting a Pasteur pipette through the IL layer and applying suction. The amount of extracted FFA can then be determined by evaporating the chloroform. On the other hand, the IL might be better applied in acidolysis reactions since the FFA that would be used for substitutions with the TAG would mostly remain in the IL. However, the FAs of the TAG substituted with the FFA in the IL would have a high percentage remaining in the IL. To investigate this, a similar experimental setup as documented in this Thesis could be used but with a pure TAG replacing LA. This would help determine the percentage of TAG settling into the IL phase relative to the HX phase.

Construction of phase diagrams at higher temperatures may prove useful for further assessment of the IL for enzymatic reactions. The solubility of LA in HX increases at

higher temperatures (Cepeda et al., 2009) but the solubility of IL with HX also increases (Anderson et al., 2009; Makowska et al., 2010). Therefore, determining the amount of LA in HX at higher temperatures can help show which opposing force is stronger. Experiments could be constructed so that the system is initially sampled at a higher temperature and then again after a set amount of time, when the system cools down to room temperature.

The high viscosity of the ILs alone is proposed to act as a method to support free enzymes during reactions. However, by adding a solvent or water layer to the system and allowing equilibration by vortexing, the enzymes might be distributed in any of the different layers. The dispersal of enzymes from the IL would not allow subsequent use and therefore, further studies to determine where enzymes in IL may partition after the addition of different solvents or water is necessary. A comparison between the efficacy of free enzymes in IL with free enzymes in solvent, the lifecycle of the free enzymes in the IL compared to that of immobilized enzymes and the possible toxicity of the IL to the enzyme lifecycle are all related topics that should be considered.

The research shown here was conducted to help pave a basis to understanding and solving a bigger question. The potential ability to employ an IL as a medium for subsequent reactions using free enzymes is of great significance. Where many studies have concentrated on devising techniques to immobilize enzymes on solid support systems, this research shows that the IL [P_{66614}] [Cl] can potentially be used as a supportive liquid medium for free enzymes to catalyze reactions. However, a method that would allow the full extraction of the products without affecting the IL enzyme complex is necessary to deem the IL a fully successful supportive liquid medium.

BIBLIOGRAPHY

Abu-Eishah, S. I. (2011). Ionic Liquids Recycling for Reuse. In *Ionic Liquids – Classes and Properties (Edited by Scott T. Handy)* (pp. 239–272). InTech 2011.

Ackelsberg, O. J. (1958). Fat splitting. *J Am Oil Chem Soc Journal of the American Oil Chemists Society*, *35*(11), 635–640.

Aminabhavi, T. M., Patil, V. B., Aralaguppi, M. I., & Phayde, H. T. S. (1996). Density , Viscosity , and Refractive Index of the Binary Mixtures of Cyclohexane with Hexane , Heptane , Octane , Nonane , and Decane at (298 . 15 , 303 . 15 , and 308 . 15) K, 521–525.

Anderson, K., Rodríguez, H., & Seddon, K. R. (2009). Phase behaviour of trihexyl(tetradecyl)phosphonium chloride, nonane and water. *Green Chemistry*, *11*(6), 780. doi:10.1039/b821925g

Atefi, F., Garcia, M. T., Singer, R. D., & Scammells, P. J. (2009). Phosphonium ionic liquids: design, synthesis and evaluation of biodegradability. *Green Chemistry*, *11*(10), 1595. doi:10.1039/b913057h

Bucolo, G., & David, H. (1973). Quantitative Determination of Serum Triglycerides by the Use of Enzymes. *Clinical Chemistry* , *19* (5), 476–482. Retrieved from http://www.clinchem.org/content/19/5/476.abstract

Budge, S. M., Iverson, S. J., & Koopman, H. N. (2006). Studying Trophic Ecology in Marine Ecosystems Using Fatty Acids: a Primer on Analysis and Interpretation. *Marine Mammal Science*, *22*(4), 759–801. doi:10.1111/j.1748-7692.2006.00079.x

Cepeda, E. A., Bravo, R., & Calvo, B. (2009). Solubilities of Lauric Acid in n-Hexane, Acetone, Propanol, 2-Propanol, 1-Bromopropane, and Trichloroethylene from (279.0 to 315.3) K. *Journal of Chemical & Engineering Data*, *54*(4), 1371–1374. doi:10.1021/je800739y

Chen, C. C., Simoni, L. D., Brennecke, J. F., & Stadtherr, M. A. (2008). Correlation and Prediction of Phase Behavior of Organic Compounds in Ionic Liquids Using the Nonrandom Two-Liquid Segment Activity Coefficient Model. *Industrial & Engineering Chemistry Research*, *47*(18), 7081–7093. doi:10.1021/ie800048d

Chen, Y. H., Chen, J. H., & Luo, Y.-M. (2012). Complementary biodiesel combination from tung and medium-chain fatty acid oils. *Renewable Energy*, *44*, 305–310. doi:10.1016/j.renene.2012.01.098

Chowdhury, S. A., Scott, J. L., & MacFarlane, D. R. (2008). Ternary mixtures of phosphonium ionic liquids + organic solvents + water. *Pure and Applied Chemistry*, *80*(6), 1325–1335. doi:10.1351/pac200880061325

Christie, W. W. (2002). Mass Spectrometry of Fatty Acid Derivatives (Vol. 104, pp. 36–43). doi:10.1002/1438-9312(200201)104:1<36::AID-EJLT111136>3.0.CO;2-W

Christie, W. W., & Han, X. (2010). Lipid Analysis: Isolation, Separation, Identification and Lipidomic Analysis. 4. *The Oily Press, Bridgwater, England*.

Clark, T. J., & Bunch, J. E. (1997). Determination of Volatile Acids in Tobacco, Tea, and Coffee Using Derivatization—Purge and Trap Gas Chromatography—Selected Ion Monitoring Mass Spectrometry. *Journal of Chromatographic Science*, *35*(5), 206–208. doi:10.1093/chromsci/35.5.206

Croes, K., Casteels, M., Asselberghs, S., Herdewijn, P., Mannaerts, G. P., & Van Veldhoven, P. P. (1997). Formation of a 2-methyl-branched fatty aldehyde during peroxisomal α-oxidation. *FEBS Letters*, *412*(3), 643–645. doi:10.1016/S0014-5793(97)00856-9

Cull, S. G., Holbrey, J. D., Vargas-Mora, V., Seddon, K. R., & Lye, G. J. (2000). Room-temperature ionic liquids as replacements for organic solvents in multiphase bioprocess operations. *Biotechnology and Bioengineering*, *69*(2), 227–233. doi:10.1002/(SICI)1097-0290(20000720)69:2<227::AID-BIT12>3.0.CO;2-0

David, F., Sandra, P., & Vickers, A. K. (2005). Column selection for the analysis of fatty acid methyl esters. *Food Analysis Application. Palo Alto, CA: Agilent Technologies*.

Davis James H., J., & Fox, P. A. (2003). From curiosities to commodities: ionic liquids begin the transition. *Chemical Communications*, (11), 1209–1212. doi:10.1039/B212788A

de los Ríos, A. P., Hernández-Fernández, F. J., Rubio, M., Tomás-Alonso, F., Gómez, D., & Víllora, G. (2008). Prediction of the selectivity in the recovery of transesterification reaction products using supported liquid membranes based on ionic liquids. *Journal of Membrane Science*, *307*(2), 225–232. doi:10.1016/j.memsci.2007.09.019

De Roos, N., Katan, M., & Schouten, E. (2001). Consumption of a solid fat rich in lauric acid results in a more favorable serum lipid profile in healthy men and women than consumption of a solid fat rich in trans-fatty acids. *The Journal of Nutrition*, *131*(2), 242–245.

Diedenhofen, M., Eckert, F., & Klamt, A. (2003). Prediction of Infinite Dilution Activity Coefficients of Organic Compounds in Ionic Liquids Using COSMO-RS†. *Journal of Chemical & Engineering Data*, *48*(3), 475–479. doi:10.1021/je025626e

Domańska, U., & Królikowski, M. (2012). Extraction of butan-1-ol from water with ionic liquids at T=308.15K. *The Journal of Chemical Thermodynamics*, *53*, 108–113. doi:10.1016/j.jct.2012.04.017

Earle, M. J., Hardacre, C., Ramani, A., Roberston, A. J., & Seddon, K. R. (2003, March 13). Composition comprising phosphonium salts and their use. Google Patents. Retrieved from http://www.google.com/patents/WO2003020843A1?cl=en

Eike, D. M., Brennecke, J. F., & Maginn, E. J. (2004). Predicting Infinite-Dilution Activity Coefficients of Organic Solutes in Ionic Liquids. *Industrial & Engineering Chemistry Research*, *43*(4), 1039–1048. doi:10.1021/ie034152p

Ferreira, A. F., Simões, P. N., & Ferreira, A. G. M. (2012). Quaternary phosphonium-based ionic liquids: Thermal stability and heat capacity of the liquid phase. *The Journal of Chemical Thermodynamics*, *45*(1), 16–27. doi:10.1016/j.jct.2011.08.019

Fraser, K. J., & MacFarlane, D. R. (2009). Phosphonium-Based Ionic Liquids: An Overview. *Australian Journal of Chemistry*, *62*(4), 309. doi:10.1071/CH08558

Freire, M. G., Neves, C. M. S. S., Marrucho, I. M., Coutinho, J. a P., & Fernandes, A. M. (2010). Hydrolysis of tetrafluoroborate and hexafluorophosphate counter ions in imidazolium-based ionic liquids. *The Journal of Physical Chemistry. A*, *114*(11), 3744–9. doi:10.1021/jp903292n

Fu, J. K., & Luthy, G. R. (1986). Aromatic compound solubility in solvent/water mixtures. *J Environ Eng Journal of Environmental Engineering*, *112*, 328–345.

Gao, Y., Chen, W., Lei, H., Liu, Y., Lin, X., & Ruan, R. (2009). Optimization of transesterification conditions for the production of fatty acid methyl ester (FAME) from Chinese tallow kernel oil with surfactant-coated lipase. *Biomass and Bioenergy*, *33*(2), 277–282. doi:10.1016/j.biombioe.2008.05.013

Gardas, R. L., & João, A. P. (2009). Group contribution methods for the prediction of thermophysical and transport properties of ionic liquids. *AIC AIChE Journal*, *55*(5), 1274–1290.

Ghaly, A. E., Dave, D., Brooks, M. S., & Budge, S. M. (2010). Production of biodiesel by enzymatic transesterification: review. *American Journal of Biochemistry and Biotechnology*, *6*(2), 54.

Ghioni, C., Bell, J. G., & Sargent, J. R. (1996). Polyunsaturated fatty acids in neutral lipids and phospholipids of some freshwater insects. *Comparative Biochemistry and Physiology Part B: Biochemistry and Molecular Biology*, *114*(2), 161–170. doi:10.1016/0305-0491(96)00019-3

Haas, M. J., Cichowicz, D. J., Jun, W., & Scott, K. (1995). The enzymatic hydrolysis of triglyceride-phospholipid mixtures in an organic solvent. *Journal of the American Oil Chemists' Society*, *72*(5), 519–525. doi:10.1007/BF02638851

Hamam, F., & Shahidi, F. (2005). Enzymatic incorporation of capric acid into a single cell oil rich in docosahexaenoic acid and docosapentaenoic acid and oxidative stability of the resultant structured lipid. *Food Chemistry*, *91*(4), 583–591. doi:10.1016/j.foodchem.2004.05.024

Hernández-Fernández, F. J., de los Ríos, A. P., Gómez, D., Rubio, M., Tomás-Alonso, F., & Víllora, G. (2008). Ternary liquid–liquid equilibria for mixtures of an ionic liquid+n-hexane+an organic compound involved in the kinetic resolution of rac-1-phenyl ethanol (rac-1-phenyl ethanol, vinyl propionate, rac-1-phenylethyl propionate or propionic acid) at 298.2K and. *Fluid Phase Equilibria*, *263*(2), 190–198. doi:10.1016/j.fluid.2007.10.011

Hilditch, T. P., & Williams, P. N. (1964). The chemical constitution of natural fats. *The Chemical Constitution of Natural Fats.*, (4th edition).

Hoerr, C. W., & Harwood, H. J. (1951). Solubilities of high molecular weight aliphatic compounds in n-hexane. *The Journal of Organic Chemistry*, *16*(5), 779–791. doi:10.1021/jo01145a020

Ibrahim, A., & Ghannoum, M. (1996). Chromatographic Analysis of Lipids. In R. Prasad (Ed.), *Manual on Membrane Lipids* (pp. 52–79). Springer Berlin Heidelberg. doi:10.1007/978-3-642-79837-5_4

Ichihara, K., & Fukubayashi, Y. (2010). Preparation of fatty acid methyl esters for gas-liquid chromatography. *Journal of Lipid Research* , *51* (3), 635–640. doi:10.1194/jlr.D001065

Iwata, T., Inoue, K., Nakamura, M., & Yamaguchi, M. (1992). Simple and highly sensitive determination of free fatty acids in human serum by high performance liquid chromatography with fluorescence detection. *Biomedical Chromatography*, *6*(3), 120–123. doi:10.1002/bmc.1130060304

Kragl, U., Eckstein, M., & Kaftzik, N. (2002). Enzyme catalysis in ionic liquids. *Current Opinion in Biotechnology*, *13*(6), 565–71. Retrieved from http://www.ncbi.nlm.nih.gov/pubmed/12482515

Krygier, K., Sosulski, F., & Hogge, L. (1982). Free, esterified, and insoluble-bound phenolic acids. 1. Extraction and purification procedure. *Journal of Agricultural and Food Chemistry*, *30*(2), 330–334. doi:10.1021/jf00110a028

Lago, S., Rodríguez, H., Khoshkbarchi, M. K., Soto, A., & Arce, A. (2012). Enhanced oil recovery using the ionic liquid trihexyl(tetradecyl)phosphonium chloride: phase behaviour and properties. *RSC Advances*, *2*(25), 9392. doi:10.1039/c2ra21698a

Lau, R. M., van Rantwijk, F., Seddon, K. R., & Sheldon, R. A. (2000). Lipase-catalyzed reactions in ionic liquids. *Organic Letters*, *2*(26), 4189–91. Retrieved from http://www.ncbi.nlm.nih.gov/pubmed/11150196

Makowska, A., Siporska, A., Oracz, P., & Szydłowski, J. (2010). Miscibility of Trihexyl(tetradecyl)phosphonium Chloride with Alkanes. *Journal of Chemical & Engineering Data*, *55*(8), 2829–2832. doi:10.1021/je9010079

Marina, A. ., Che Man, Y. ., Nazimah, S. A. ., & Amin, I. (2009). Chemical Properties of Virgin Coconut Oil. *Journal of the American Oil Chemists' Society*, *86*(4), 301–307. doi:10.1007/s11746-009-1351-1

Marták, J., & Schlosser, Š. (2006). Phosphonium ionic liquids as new, reactive extractants of lactic acid. *Chemical Papers*, *60*(5), 395–398. doi:10.2478/s11696-006-0072-2

Matyash, V., Liebisch, G., Kurzchalia, T. V, Shevchenko, A., & Schwudke, D. (2008). Lipid extraction by methyl-tert-butyl ether for high-throughput lipidomics. *Journal of Lipid Research*, *49*(5), 1137–1146. doi:10.1194/jlr.D700041-JLR200

McNeill, G. P., Shimizu, S., & Yamane, T. (1991). High-Yield Enzymatic Glycerolysis of Fats and Oils, *68*(I).

Metcalfe, L. D., & Schmitz, A. A. (1961). The Rapid Preparation of Fatty Acid Esters for Gas Chromatographic Analysis. *Analytical Chemistry*, *33*(3), 363–364. doi:10.1021/ac60171a016

Murty, V. R., Bhat, J., & Muniswaran, P. K. a. (2002). Hydrolysis of oils by using immobilized lipase enzyme: A review. *Biotechnology and Bioprocess Engineering*, *7*(2), 57–66. doi:10.1007/BF02935881

Ngaosuwan, K., Suwannakarn, K., J.G., G. J., Praserthdam, P., & Lotero, E. (2009). Hydrolysis of triglycerides using solid acid catalysts. *Ind. Eng. Chem. Res. Industrial and Engineering Chemistry Research*, *48*(10), 4757–4767.

Nicotera, I., Oliviero, C., Henderson, W. a, Appetecchi, G. B., & Passerini, S. (2005). NMR investigation of ionic liquid-LiX mixtures: pyrrolidinium cations and TFSI-anions. *The Journal of Physical Chemistry. B*, *109*(48), 22814–9. doi:10.1021/jp053799f

Noureddini, H., Teoh, B. C., & Davis Clements, L. (1992). Densities of vegetable oils and fatty acids. *Journal of the American Oil Chemists Society*, *69*(12), 1184–1188. doi:10.1007/BF02637677

Nyrén, V., Ernst, B., Veikko, P., Bengt-Olov, M., Veige, S., & Diczfalusy, E. (1958). The Ionization Constant, Solubility Product, and Solubility of Lauric and Myristic Acids. *Acta Chem.Scand.Acta Chemica Scandinavica*, *12*, 1305–1311.

Pàdua, A. a H., Costa Gomes, M. F., & Canongia Lopes, J. N. a. (2007). Molecular solutes in ionic liquids: A structural perspective. *Accounts of Chemical Research*, *40*(11), 1087–1096.

Parfene, G., Horincar, V., Tyagi, A., Malik, A., & Bahrim, G. (2013). Production of medium chain saturated fatty acids with enhanced antimicrobial activity from crude coconut fat by solid state cultivation of Yarrowia lipolytica. *Food Chemistry*, *136*(3-4), 1345–9. doi:10.1016/j.foodchem.2012.09.057

Ramnial, T., Ino, D. D., & Clyburne, J. a C. (2005). Phosphonium ionic liquids as reaction media for strong bases. *Chemical Communications (Cambridge, England)*, (3), 325–7. doi:10.1039/b411646a

Rogers, R. D., & Seddon, K. R. (2003). Ionic liquids--solvents of the future? *Science (New York, N.Y.)*, *302*(5646), 792–3. doi:10.1126/science.1090313

Serri, N. A., Kamarudin, A. H., & Abdul Rahaman, S. N. (2008). Preliminary studies for production of fatty acids from hydrolysis of cooking palm oil using C. rugosa lipase. *Journal of Physical Science*, *19*(1), 79–88.

Sheldon, R. A. (2005). Green solvents for sustainable organic synthesis: state of the art. *Green Chemistry*, *7*(5), 267–278. doi:10.1039/B418069K

Sheldon, R. A., Lau, R. M., Sorgedrager, M. J., van Rantwijk, F., & Seddon, K. R. (2002). Biocatalysis in ionic liquids. *Green Chemistry*, *4*(2), 147–151. doi:10.1039/b110008b

Sigma-Aldrich. (2014a). *Dodecanoic acid*. Retrieved May 27, 2014, from http://www.sigmaaldrich.com/catalog/product/aldrich/l556?lang=en&region=CA

Sigma-Aldrich. (2014b). *n-Hexane Physical Properties*. Retrieved May 27, 2014, from http://www.sigmaaldrich.com/chemistry/solvents/hexane-center/physical-properties.html

Sowmiah, S., Srinivasadesikan, V., Tseng, M.-C., & Chu, Y.-H. (2009). *On the chemical stabilities of ionic liquids. Molecules (Basel, Switzerland)* (Vol. 14, pp. 3780–813). doi:10.3390/molecules14093780

Sparkman, D., Penton, Z., & Kitson, F. (2011). Internal Standard Method. In *Gas Chromatography and Mass Spectrometry: A Practical Guide* (Second., pp. 214–216). Oxford, UK.

Stojanovic, A., Kogelnig, D., Fischer, L., Hann, S., Galanski, M., Groessl, M., … Keppler, B. K. (2010). Phosphonium and Ammonium Ionic Liquids with Aromatic Anions: Synthesis, Properties, and Platinum Extraction. *Australian Journal of Chemistry*, *63*(3), 511. doi:10.1071/CH09340

Stojanovic, A., Morgenbesser, C., Kogelnig, D., Krachler, R., & Keppler, B. K. (2011). Quaternary Ammonium and Phosphonium Ionic Liquids in Chemical and Environmental Engineering.

Strem Chemicals Inc. (2014). *MSDS, Trihexyl(tetradecyl)phosphonium chloride*. Retrieved June 01, 2014, from http://www.strem.com/catalog/msds/15-6382

Temme, E. H. M., Mensink, R. P., & Hornstra, G. (1999). Effects of Diets Enriched in Lauric, Palmitic or Oleic Acids on Blood Coagulation and Fibrinolysis. *Thrombosis and Haemostasis*, *81*(2), 259–263. Retrieved from http://www.schattauer.de/t3page/1214.html?manuscript=4762&L=1

Temme, H., Dethloff, O., Pitner, W.-R., Fischer, S., Scheurich, R., Schulte, M., & Niemeyer, B. (2012). Identification of suitable ionic liquids for application in the enzymatic hydrolysis of rutin by an automated screening. *Applied Microbiology and Biotechnology*, *93*(6), 2301–8. doi:10.1007/s00253-011-3749-6

Tizol-Correa, R., Carreón-Palau, L., Arredondo-Vega, B. O., Murugan, G., Torrentera, L., Maldonado-Montiel, T. D. N. J., & Maeda-Martínez, A. M. (2006). Fatty Acid Composition of Artemia (Branchiopoda: Anostraca) Cysts from Tropical Salterns of Southern México and Cuba. *Journal of Crustacean Biology*, *26*(4), 503–509. doi:10.2307/4094180

Tseng, M. C., Kan, H. C., & Chu, Y. H. (2007). Reactivity of trihexyl(tetradecyl)phosphonium chloride, a room-temperature phosphonium ionic liquid. *Tetrahedron Letters*, *48*(52), 9085–9089. doi:10.1016/j.tetlet.2007.10.131

Tsonopoulos, C., & Wilson, G. M. (1983). High-temperature mutual solubilities of hydrocarbons and water. Part I: Benzene, cyclohexane and n-hexane. *AIChE Journal*, *29*(6), 990–999. doi:10.1002/aic.690290618

Visser, A. E., Swatloski, R. P., Reichert, W. M., Griffin, S. T., & Rogers, R. D. (2000). Traditional Extractants in Nontraditional Solvents: Groups 1 and 2 Extraction by Crown Ethers in Room-Temperature Ionic Liquids†. *Industrial & Engineering Chemistry Research*, *39*(10), 3596–3604. doi:10.1021/ie000426m

Visser, A. E., Swatloski, R. P., Reichert, W. M., Mayton, R., Sheff, S., Wierzbicki, A., … Rogers, R. D. (2001). Task-specific ionic liquids for the extraction of metal ions from aqueous solutions. *Chemical Communications*, (1), 135–136. doi:10.1039/B008041L

Wasserscheid, P., & Keim, W. (2000). Ionic liquids-new “solutions” for transition metal catalysis. *Angewandte Chemie*, *39*(21), 3772–3789.

Young, F. V. (1983). Palm Kernel and coconut oils: Analytical characteristics, process technology and uses. *Journal of the American Oil Chemists' Society*, *60*(2), 374–379. doi:10.1007/BF02543521

Yow, C. J., & Liew, K. Y. (1999). Hydrolysis of palm oil catalyzed by macroporous cation-exchanged resin. *Journal of the American Oil Chemists' Society*, *76*(4), 529–533. doi:10.1007/s11746-999-0036-0

Zaidi, A., Gainer, J. ., Carta, G., Mrani, A., Kadiri, T., Belarbi, Y., & Mir, A. (2002). Esterification of fatty acids using nylon-immobilized lipase in n-hexane: kinetic parameters and chain-length effects. *Journal of Biotechnology*, *93*(3), 209–216. doi:10.1016/S0168-1656(01)00401-1

Zhao, D., Wu, M., Kou, Y., & Min, E. (2002). Ionic liquids: applications in catalysis. *Catalysis Today*, *74*(1-2), 157–189. doi:10.1016/S0920-5861(01)00541-7

APPENDIX A

Enzymatic runs

Control: Lipase powder enzyme (free enzyme) from *Aspergillus niger* (Amano A) was generously gifted by Amano Enzymes (Troy, VA).

In triplicate: 32 mg "Amano A" enzyme, 0.1 g water, 0.5 g canola oil and 2 ml hexane were added to a test tube following ratios provided by McNeill et al. (1991). A 5 mm magnetic stir bar was added and the samples placed on a magnetic hot plate. The temperature was raised to 45 °C and the sample was stirred at approximately 800 rpm for 12 hrs as per reported optimal enzymatic activity conditions (Haas et al., 1995; Murty et al., 2002).

A 10 ml mixture of ethanol and acetone was then added to stop the reaction (1:1 v/v) (Hamam & Shahidi, 2005). 10 ml hexane was then added to the mixture followed by vortexing for 2 min and centrifuging at 2000g for 5 min. The top layer (hexane) was extracted to a separate test tube and a scoop of anhydrous sodium hydroxide was added. After settling, the solvent was removed to a pre-weighed test tube and evaporated in the water bath at 34 °C under a steady stream of nitrogen. The sample was then dissolved in chloroform at a concentration of 250 mg lipid/ml of chloroform.

Trial enzymatic run in IL: In triplicate: 1 ml [P_{66614}] [Cl] was added to a test tube containing 32 mg "Amano A" enzyme, 0.1 g water and a magnetic stir bar. 0.5 g canola oil was added on top and the sample placed on a magnetic hot plate. The temperature was raised to 45 °C and stirred at approximately 800 rpm for 12 hrs.

After the run was completed, 1 ml water was added which formed a layer below the IL. This was followed with 5 ml hexane which was allowed to settle on top of the IL for 10 minutes before being extracted to a separate test tube (no vortexing was done as the hexane

would mix with the IL and disrupt the enzymes). Although the enzymes were suspended in the IL layer, the mixture of ethanol and acetone was added to the extracted hexane to be sure that if any traces of enzyme were extracted, the reaction would be inactivated. The rest of the procedure done in the control run was then followed.

TLC: TLC silica gels plates (200 × 200 mm; 60 Å mean pore diameter, 10–12 μm mean particle size, 250 μm layer thickness) purchased from Merck KGaA (Bellerica, MA) were used to determine the results of the hydrolysis reactions. The developing sides of the plates were saturated with ethyl acetate and then allowed to dry before placing in an oven for an hour at 100 °C. Standards were dissolved in chloroform at a concentration of 50 mg lipid/ml of chloroform. The samples and standards were streaked on the silica gel plates with a 25μl micropipette. The silica gel plates were then developed using a mixture solvent of 80:20:1 (v/v/v, hexane/diethyl ether/acetic acid) and then allowed to dry before being evenly sprayed with 0.2% dichloroflourocine in ethanol. The bands were then observed under ultra-violet (254 nm) short wave light.

APPENDIX B

Calculating the correction factor

The detector response to LA FAME and the IS (Methyl tricosanoate) is not the same. The concentration ratios of IS and of LA FAME are not equal to the ratio of their respective peak areas. A correction factor was calculated therefore to account for the difference in peak area ratios. The calculation was done by taking a known mass of IS = 101.8 mg and a known mass of LA FAME = 104.1 mg and injecting into the GC 6 times following the same method described in section 3.2.5 and an average area count for both the IS and LA FAME was calculated.

$$CF = \frac{m_{IS}}{m_{LA}} \times \frac{Avg_{LA}}{Avg_{IS}}$$

Where CF = the correction factor

m_{IS} = known mass of IS

m_{LA} = known mass of LA FAME

Avg_{LA} = average peak area of LA FAME

Avg_{IS} = average peak area of IS

The CF was calculated to be = 0.702378 and was applied to each FAME sample (Sparkman et al., 2011).

APPENDIX C

Mass fraction data

A-1: Average mass fraction values of LA from the bottom and top phase at different concentrations of LA/HX (not corrected for LA removed). Included are the standard deviations for LA in each phase and the percentages.

Total LA added (mg)	LA/HX volume (ml)	LA (Top)	LA (Bottom)	LA SD (Top)	LA % SD (Top)	LA SD (Bottom)	LA % SD (Bottom)
4	**4**	0.0001	0.0024	6.18E-06	4.53E+00	9.74E-05	4.06E+00
14	**5**	0.0003	0.0076	5.01E-05	1.59E+01	1.25E-04	1.64E+00
24	**6**	0.0007	0.0124	2.31E-04	3.53E+01	2.78E-04	2.25E+00
34	**7**	0.0010	0.0168	3.67E-05	3.59E+00	3.78E-04	2.25E+00
40	**4**	0.0007	0.0183	2.83E-04	4.04E+01	3.94E-04	2.15E+00
60	**5**	0.0023	0.0243	9.54E-04	4.14E+01	8.70E-04	3.58E+00
80	**6**	0.0049	0.0259	6.31E-06	1.28E-01	4.80E-04	1.85E+00
80 (outlier)	**6**	0.0095	0.0209	n/a	n/a	n/a	n/a
100 (Single phase C)	**7**	n/a	0.0176	n/a	n/a	6.68E-04	3.80E+00
100 (Single phase M)	**7**	n/a	0.0178	n/a	n/a	6.46E-04	3.63E+00
0 (Blank)	**4**	0	0	0	0	0	0

A-2: Average mass fraction values of IL from the bottom and top phase at different concentrations of LA/HX (not corrected for LA removed) corrected for sources of error. Included are the standard deviations for IL in each phase and the percentages.

Total LA added (mg)	LA/HX volume (ml)	IL (Top)	IL (Bottom)	IL SD (Top)	IL % SD (Top)	IL SD (Bottom)	IL %SD (Bottom)
4	**4**	0.0297	0.4465	1.13E-03	3.80E+00	9.81E-04	2.20E-01
14	**5**	0.0428	0.4079	8.93E-03	2.09E+01	8.35E-03	2.05E+00
24	**6**	0.0345	0.3914	4.98E-03	1.44E+01	8.78E-03	2.24E+00
34	**7**	0.0357	0.3657	5.70E-03	1.60E+01	9.28E-03	2.54E+00
40	**4**	0.0484	0.3782	2.36E-03	4.87E+00	1.16E-03	3.07E-01
60	**5**	0.0582	0.3212	1.27E-03	2.18E+00	2.76E-03	8.61E-01
80	**6**	0.0847	0.2379	1.32E-02	1.56E+01	1.11E-02	4.66E+00
80 (outlier)	**6**	0.1071	0.2074	n/a	n/a	n/a	n/a
100 (Single phase C)	**7**	n/a	0.1369	n/a	n/a	4.22E-03	3.08E+00
100 (Single phase M)	**7**	n/a	0.1382	n/a	n/a	1.24E-02	9.00E+00
0 (Blank)	**4**	0.0104	0.4652	8.77E-05	8.43E-01	2.37E-03	5.09E-01

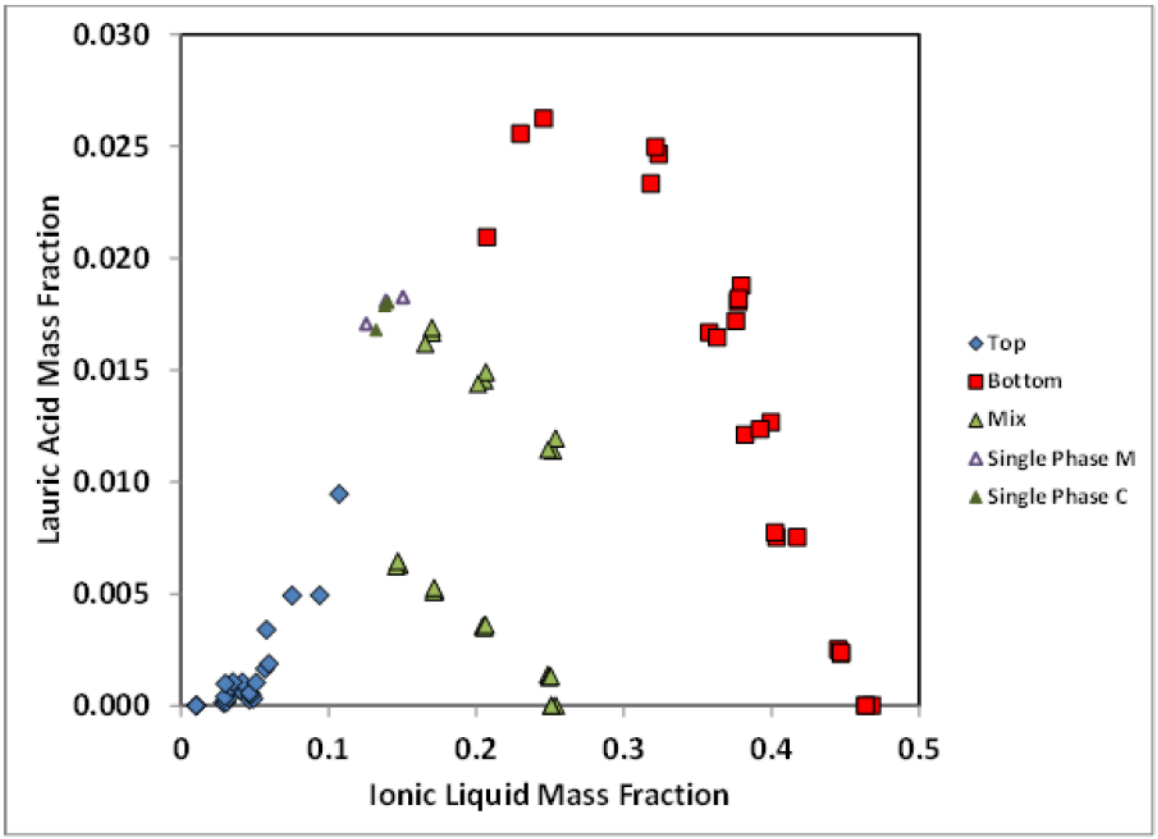

B-1: Mass fraction phase diagram of all the experimental data points collected for LA+IL corrected for sources of error. The experimental points are taken from the collected data resulting from Series #1 and Series #2 illustrated in Table 3-2 and Table 3-3. Included are the measured single phase points as well as the mix points.

A-3: Non-average experimental mass fraction values of LA mixtures, top and bottom phases corrected for possible sources of error. Total LA is (not corrected for LA removed from system).

Total LA added (mg)	**LA/HX volume (ml)**	**Top (LA) Mass fraction**	**Mix (LA) Mass fraction**	**Bottom (LA) Mass fraction**
4	**4**	0.0001	0.0014	0.0025
		0.0001	0.0013	0.0023
		0.0001	0.0013	0.0024
14	**5**	0.0004	0.0036	0.0075
		0.0003	0.0035	0.0075
		0.0003	0.0036	0.0077
24	**6**	0.0004	0.0051	0.0127
		0.0007	0.0051	0.0121
		0.0008	0.0053	0.0124
34	**7**	0.0010	0.0063	0.0167
		0.0011	0.0062	0.0165
		0.0010	0.0065	0.0172
40	**4**	0.0005	0.0114	0.0180
		0.0006	0.0119	0.0188
		0.0010	0.0114	0.0182
60	**5**	0.0017	0.0145	0.0247
		0.0019	0.0149	0.0250
		0.0034	0.0144	0.0233
80	**6**	0.0049	0.0167	0.0256
		0.0049	0.0169	0.0262
		0.0095	0.0162	0.0209
100 (Single phase M)	**7**	n/a	0.0183	n/a
		n/a	0.0181	n/a
		n/a	0.0171	n/a
100 (Single phase C)	**7**	n/a	0.0179	n/a
		n/a	0.0180	n/a
		n/a	0.0168	n/a
0 (Blank)	**4**	0	0	0
		0	0	0
		0	0	0

A-4: Non-average experimental mass fraction values of IL mixtures, top and bottom phases corrected for sources of error. Total LA is (not corrected for LA removed from system).

Total LA added (mg) (not including extracted)	LA/HX volume (ml)	Top (IL) Mass fraction	Mix (IL) Mass fraction	Bottom (IL) Mass fraction
4	**4**	0.0295	0.2486	0.4454
		0.0287	0.24929	0.4470
		0.0309	0.2506	0.4471
14	**5**	0.0326	0.2047	0.4175
		0.0465	0.2055	0.4036
		0.0493	0.2063	0.4026
24	**6**	0.0299	0.1724	0.3996
		0.0398	0.1712	0.3822
		0.0338	0.1716	0.3924
34	**7**	0.0416	0.1481	0.3578
		0.0353	0.1458	0.3633
		0.0302	0.1469	0.3759
40	**4**	0.0479	0.2521	0.3774
		0.0464	0.2538	0.3796
		0.0510	0.2488	0.3778
60	**5**	0.0571	0.2056	0.3237
		0.0596	0.2066	0.3216
		0.0580	0.2012	0.3183
80	**6**	0.0940	0.1701	0.2301
		0.0754	0.1702	0.2458
		0.1072	0.1655	0.2074
100 (Single phase M)	**7**	n/a	0.1503	n/a
		n/a	0.1388	n/a
		n/a	0.1254	n/a
100 (Single phase C)	**7**	n/a	0.1381	n/a
		n/a	0.1404	n/a
		n/a	0.1322	n/a
0 (Blank)	**4**	0.0105	0.2541	0.4679
		0.0104	0.2509	0.4638
		0.0104	0.2510	0.4639

Original mass fraction values

Included here are the original mass fraction values not corrected by the addition of possible sources of error enlisted in section 4.3.

A-5: Original average mass fraction values of LA from the bottom and top phase at different concentrations of LA/HX (not corrected for LA removed). Included are the standard deviations for LA in each phase and the percentages.

Total LA added (mg)	LA/HX volume (ml)	LA (Top)	LA (Bottom)	LA SD (Top)	LA % SD (Top)	LA SD (Bottom)	LA % SD (Bottom)
4	**4**	0.0001	0.0024	6.18E-06	4.53E+00	9.74E-05	4.06E+00
14	**5**	0.0003	0.0076	5.01E-05	1.59E+01	1.25E-04	1.64E+00
24	**6**	0.0007	0.0124	2.31E-04	3.53E+01	2.78E-04	2.25E+00
34	**7**	0.0010	0.0168	3.67E-05	3.59E+00	3.78E-04	2.25E+00
40	**4**	0.0007	0.0178	2.90E-04	3.94E+01	3.75E-04	2.11E+00
60	**5**	0.0024	0.0232	9.79E-04	4.04E+01	6.93E-04	2.99E+00
80	**6**	0.0052	0.0243	8.31E-06	1.59E-01	5.48E-04	2.25E+00
80 (outlier)	**6**	0.0099	0.0199	n/a	n/a	n/a	n/a
100 (Single phase C)	**7**	n/a	0.0172	n/a	n/a	6.09E-04	3.52E+00
100 (Single phase M)	**7**	n/a	0.0188	n/a	n/a	8.36E-04	4.46E+00
0 (Blank)	**4**	0	0	0	0	0	0

A-6: Original average mass fraction values of IL from the bottom and top phase at different concentrations of LA/HX (not corrected for LA removed). Included are the standard deviations for IL in each phase and the percentages.

Total LA added (mg)	LA/HX volume (ml)	IL (Top)	IL (Bottom)	IL SD (Top)	IL % SD (Top)	IL SD (Bottom)	IL %SD (Bottom)
4	**4**	0.0297	0.4465	1.13E-03	3.80E+00	9.81E-04	2.20E-01
14	**5**	0.0428	0.4079	8.93E-03	2.09E+01	8.35E-03	2.05E+00
24	**6**	0.0345	0.3914	4.98E-03	1.44E+01	8.78E-03	2.24E+00
34	**7**	0.0357	0.3657	5.70E-03	1.60E+01	9.28E-03	2.54E+00
40	**4**	0.0510	0.3686	2.06E-03	4.04E+00	1.16E-03	6.86E-01
60	**5**	0.0613	0.3093	1.51E-03	2.46E+00	2.76E-03	4.45E-01
80	**6**	0.0897	0.2259	1.40E-02	1.56E+01	1.11E-02	6.11E+00
80 (outlier)	**6**	0.1117	0.2020	n/a	n/a	n/a	n/a
100 (Single phase C)	**7**	n/a	0.1372	n/a	n/a	3.95E-03	2.88E+00
100 (Single phase M)	**7**	n/a	0.1456	n/a	n/a	1.42E-02	9.75E+00
0 (Blank)	**4**	0.0104	0.4652	8.77E-05	8.43E-01	2.37E-03	5.09E-01

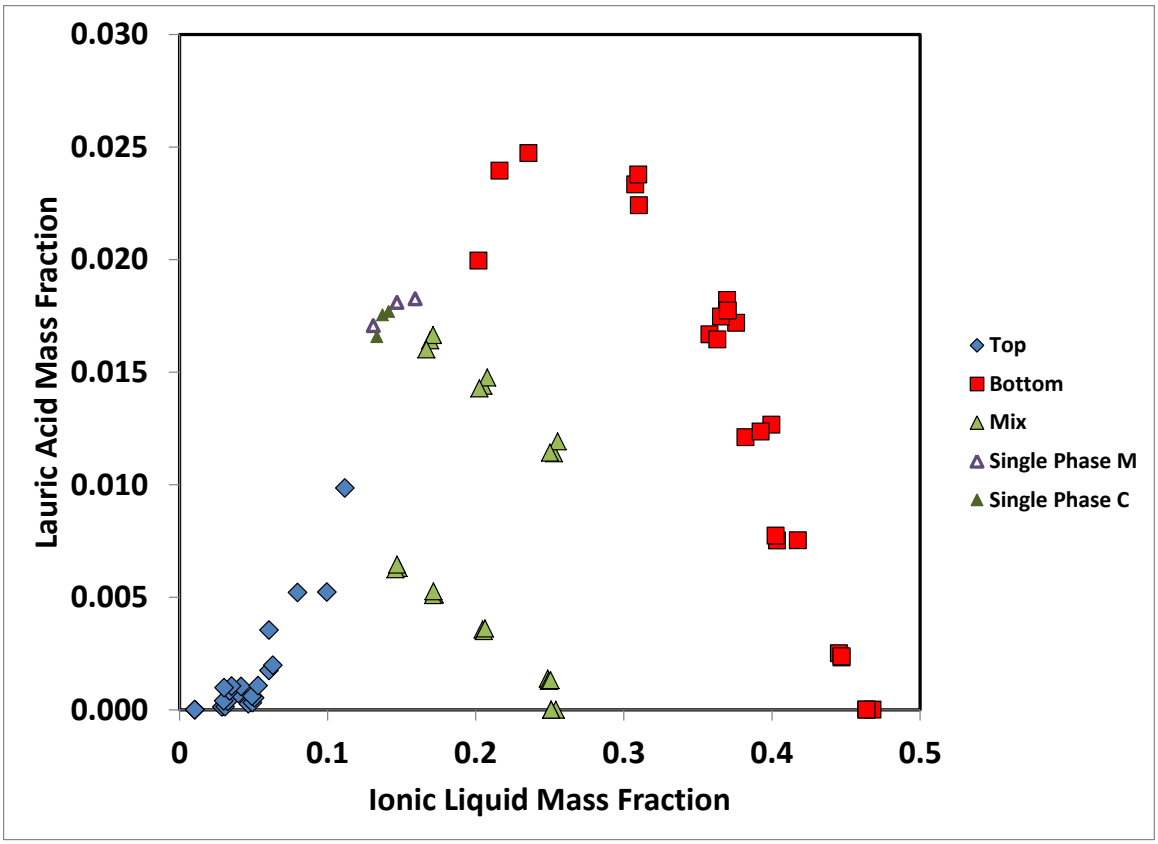

B-2: Mass fraction phase diagram of the original experimental data points collected for LA+IL without the inclusion of sources of error. The experimental points are taken from the collected data resulting from Series #1 and Series #2 illustrated in Table 3-2 and Table 3-3. Included are the measured single phase points as well as the mix points.

A-7: Original non-average experimental mass fraction values of LA mixtures, top and bottom phases not corrected for sources of error. Total LA is (not corrected for LA removed from system).

Total LA added (mg)	**LA/HX volume (ml)**	**Top (LA) Mass fraction**	**Mix (LA) Mass fraction**	**Bottom (LA) Mass fraction**
4	**4**	0.0001	0.0014	0.0025
		0.0001	0.0013	0.0023
		0.0001	0.0013	0.0024
14	**5**	0.0004	0.0036	0.0075
		0.0003	0.0035	0.0075
		0.0003	0.0036	0.0077
24	**6**	0.0004	0.0051	0.0127
		0.0007	0.0051	0.0121
		0.0008	0.0053	0.0124
34	**7**	0.0010	0.0063	0.0167
		0.0011	0.0062	0.0165
		0.0010	0.0065	0.0172
40	**4**	0.0005	0.0114	0.0175
		0.0006	0.0119	0.0182
		0.0010	0.0114	0.0177
60	**5**	0.0017	0.0144	0.0233
		0.0020	0.0148	0.0238
		0.0035	0.0143	0.0224
80	**6**	0.0052	0.0164	0.0239
		0.0052	0.0166	0.0247
		0.0099	0.0160	0.0199
100 (Single phase C)	**7**	n/a	0.0175	n/a
		n/a	0.0177	n/a
		n/a	0.0166	n/a
100 (Single phase M)	**7**	n/a	0.0193	n/a
		n/a	0.0191	n/a
		n/a	0.0178	n/a
0 (Blank)	**4**	0	0	0
		0	0	0
		0	0	0

A-8: Original non-average experimental mass fraction values of IL mixtures, top and bottom phases not corrected for sources of error. Total LA is (not corrected for LA removed from system).

Total LA added (mg) (not including extracted)	LA/HX volume (ml)	Top (IL) Mass fraction	Mix (IL) Mass fraction	Bottom (IL) Mass fraction
4	**4**	0.0295	0.2486	0.4454
		0.0287	0.24929	0.4470
		0.0309	0.2506	0.4471
14	**5**	0.0326	0.2047	0.4175
		0.0465	0.2055	0.4036
		0.0493	0.2063	0.4026
24	**6**	0.0299	0.1724	0.3996
		0.0398	0.1712	0.3822
		0.0338	0.1716	0.3924
34	**7**	0.0416	0.1481	0.3578
		0.0353	0.1458	0.3633
		0.0302	0.1469	0.3759
40	**4**	0.0508	0.2528	0.3657
		0.0491	0.2553	0.3698
		0.0532	0.2502	0.3703
60	**5**	0.0605	0.2053	0.3077
		0.0631	0.2078	0.3098
		0.0605	0.2025	0.3103
80	**6**	0.0995	0.1693	0.2162
		0.0798	0.1712	0.2357
		0.1117	0.1668	0.2020
100 (Single phase C)	**7**	n/a	0.1371	n/a
		n/a	0.1412	n/a
		n/a	0.1333	n/a
100 (Single phase M)	**7**	n/a	0.1591	n/a
		n/a	0.1468	n/a
		n/a	0.1308	n/a
0 (Blank)	**4**	0.0105	0.2541	0.4679
		0.0104	0.2509	0.4638
		0.0104	0.2510	0.4639